J Dent Sci 2010;5(1):1–7

ORIGINAL ARTICLE

The effects of splinting periodontally compromised removable partial denture abutments on bone stresses: a three-dimensional finite element study

Allahyar Geramy,[1] Mehdi Adibrad,[2] Mahasti Sahabi[3]*

[1]Department of Orthodontics, Dental School, Tehran University of Medical Science and Dental Research Center, Tehran University of Medical Sciences, Tehran, Iran
[2]Department of Periodontics, Dental School, Isfahan University of Medical Science, Isfahan, Iran
[3]Department of Prosthodontics, Dental School, Shahid Beheshti University of Medical Science, Tehran, Iran

Received: Oct 18, 2009
Accepted: Jan 21, 2010

KEY WORDS:
abutment;
biomechanics;
finite element analysis;
fixed splinting;
periodontal support;
removable partial denture

Background/purpose: Periodontally compromised abutments complicate the treatment plan of distal extension removable partial dentures. The objectives of this study were: (1) to determine if splinting a tooth with reduced bone height to a healthy one is beneficial to the weak one; (2) to investigate fixed splinting of two teeth (the first and second premolars) with various alveolar support levels on bone stress around the periodontal construction according to different crown to root ratios of the periodontally compromised abutment; and (3) to assess the efficiency of splinting in the presence of non-axial loads.
Materials and methods: Thirteen three-dimensional finite element models were designed that included the mandibular first and second premolars and the surrounding bone. Ten models were similar except for the alveolar bone height around the second premolar that had different amounts of bone resorption of 0–9 mm with splinted teeth. The last three were the same except for the teeth which were not splinted. A vertical force of 25 N was applied to each occlusal surface of the premolars. Finally, von Mises stress was evaluated at three points for all models. In the first stage, the efficiency of splinting was assessed. In the last stage, the effects of non-axial loads were evaluated in the splinted teeth models.
Results: In stage 1, it was shown that splinting could redirect the stresses to apical areas and prevented crestal bone from increased stress. In stage 2, the findings of von Mises stress in the apical area of the first premolar were almost the same in all models. In the apical area of the second premolar and the alveolar crest area, the bone stress increased when the height of the alveolar bone of the second premolar decreased. Stage 3 revealed that splinted teeth are efficient in carrying non-axial loads.
Conclusion: Splinting a very weak abutment to an adjacent healthy tooth might not be beneficial. The acceptable crown to root ratio for fixed splinting a weak abutment to an adjacent normal tooth was around 1.65–2.

*Corresponding author. Department of Orthodontics, Dental School, Tehran University of Medical Science and Dental Research Center, Tehran University of Medical Science, Tehran, Iran.
E-mail: gueramya@tums.ac.ir

Introduction

The usual treatment choices for patients with posterior edentulous ridges are cantilever fixed partial dentures (FPDs), removable partial dentures (RPDs), and implant-supported prostheses. However, anatomic considerations or financial constraints may result in considering the FPD or RPD options. Although both of these treatment modalities can provide the patient with chewing function, patients often prefer a fixed prosthesis because of perceived comfort and ease of maintenance. However, an FPD might not provide a suitable biomechanical solution because of its limited capacity to transfer occlusal forces to distant portions of the arch. This limitation is especially prominent in situations of teeth with reduced periodontal support.[1–5]

The mobility of natural teeth may increase when the supporting periodontium is lost. It is, therefore, important to reduce the deteriorating effects of the poor supporting tissues under physiologic loads in rehabilitating periodontally compromised dentition.[6] Tooth mobility in natural dentition may be eliminated or controlled by proper diagnosis and management, such as occlusal adjustments and tooth splinting in an inflammation-free environment.[6,7] For conventional FPDs, joining teeth together in a splint system is an important method used to decrease mobility in cases of reduced periodontal support.[8] Several biomechanical studies investigated the influence of bone levels and splinting on teeth with reduced periodontal support height.[9–12] The reduced bone support and unfavorable crown to root (C/R) ratio of an abutment not only reduce the area of the periodontal ligament (PDL), but also increase the leverage when a non-axial load is applied. Biomechanical factors, such as overload, leverage, torque and flexing, induce abnormal stress concentrations in the prosthesis and periodontium. Those studies demonstrated that teeth splinting can decrease both the displacement and stress concentrations.

Berg and Caputo[13] studied some aspects of stress distributions of RPDs in bilateral maxillary distal extension situations with progressive diminution of periodontal support. Itoh et al.[3] investigated the effects of periodontal support and fixed splinting on load transfer by RPDs in mandibular bilateral distal extension situations. They concluded that fixed splinting of simulated periodontally compromised abutments effectively redistributes forces to supporting structures.

Considering Ante's law [14] for FPDs, which was questioned in several studies[15,16], specific clinical guidelines for splinting are lacking. In all of those studies, the definition of a weak abutment varied among clinicians. Yang et al.[11] considered a C/R ratio of 1:0.7 for periodontally compromised abutments. In other studies,[3,9] distal abutments had mesial and distal osseous craters that were 4 mm deep. In a study by Wang et al.,[12] severely compromised periodontal involvement of the terminal abutment was defined as only one-third of the normal bone height remaining. Finally, Aydin and Tekkaya[17] assumed a C/R ratio of 1 for periodontally weak abutments. Therefore, it seems that the literature lacks criteria for periodontal involvement.

The finite element method (FEM), which was introduced to solve structural mechanical problems, has long been applied in dentistry to determine stresses and strains in dental structures caused by occlusal forces.[18] Three-dimensional (3D) FEM is a powerful tool for examining complex mechanical behaviors of prostheses and surrounding structures. Their usefulness in designing and analyzing dental restorations is well established.[19–24]

The objectives of this study were: (1) to assess the usefulness of splinting a tooth with reduced alveolar bone height to a healthy one from a stress point of view; (2) to evaluate the effects of gradual alveolar bone loss of one tooth (the second premolar) in a splinted segment of two teeth (premolars); (3) to find the greatest C/R ratio to splint a weakened tooth to a healthy one beyond which the splinting is useless; and (4) to evaluate splinted teeth when non-axial loads are applied from a stress point of view.

Material and methods

Thirteen 3D FEM models were created with a posterior mandibular segment, first and second premolars based on the average dimensions,[25] spongy, cortical bone, and PDL (Fig. 1). The normal alveolar bone model was the control, and bone loss was measured vertically from the crest of the second premolar bone level in millimeters. Each model consisted of a cancellous core surrounded by a 0.75-mm thick cortical layer. A 0.25-mm thick simplified PDL layer was modeled based on the root-form geometry of the premolar. Ten models were similar except for the alveolar bone height of the second premolar. In the first model, the alveolar bone height was normal around the second premolar (C/R ratio, 0.55). Gradual loss of alveolar bone in the second premolar increased to 9 mm in the last model (C/R ratio, 3.09). In all models, the alveolar bone height around the first premolar was kept normal. Two teeth were splinted in the crown so that they could be considered as one part with no deformation in the splint area. In the last three models, the splint was deleted from the model with 1 mm, 4 mm, and 8 mm of alveolar bone loss.

SolidWorks 2006 (Solidworks Corp., Concord, MA, USA) was selected to create the solid models. The

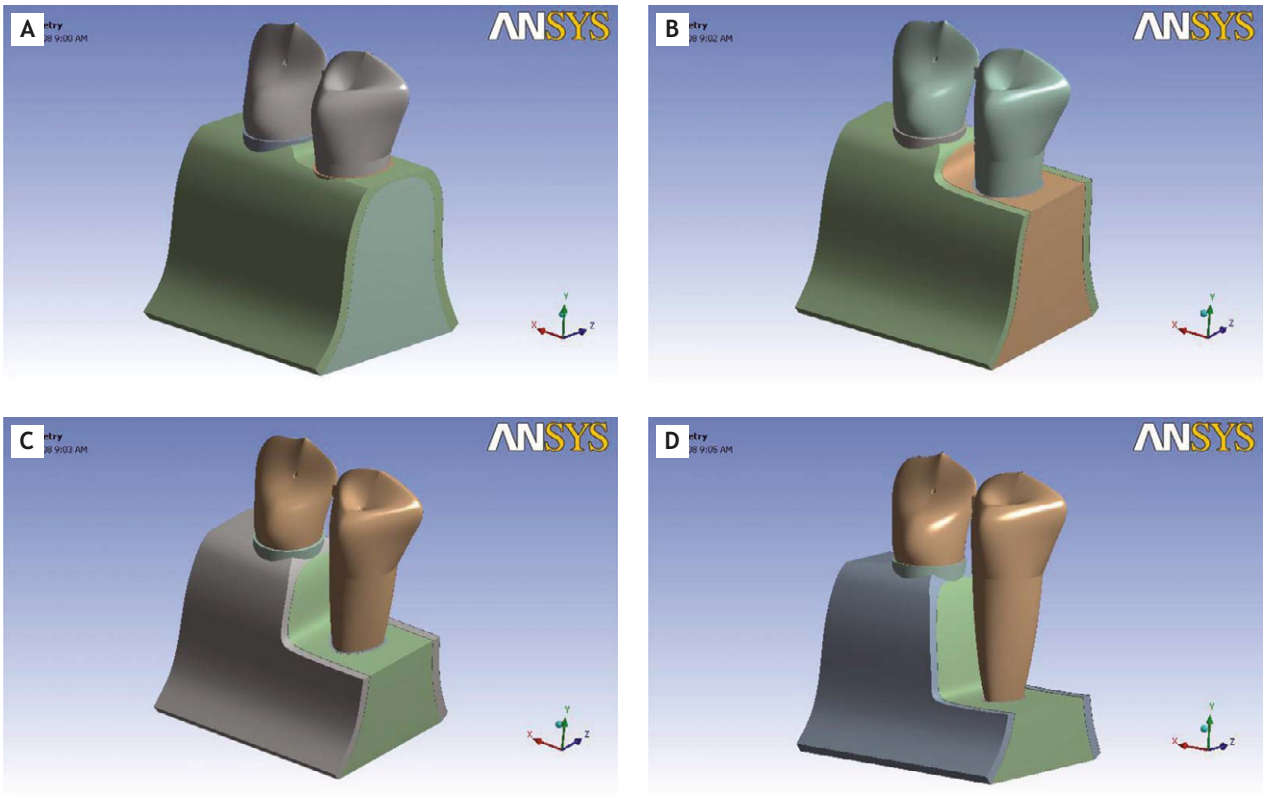

Fig. 1 Finite element models: (A) with 1 mm of bone loss in the second premolar; (B) with 3 mm of bone loss in the second premolar; (C) with 7 mm of bone loss in the second premolar; and (D) with 9 mm of bone loss in the second premolar.

models were designed in a top-to-bottom manner starting with a definition of volumes. The next step was to import the solid models into ANSYS Workbench version 11.0 (ANSYS Inc., Canonsburg, PA, USA) to construct the FEMs. All vital tissues were presumed to be elastic, homogeneous, and isotropic. The corresponding elastic properties such as Young's modulus and Poisson's ratio were determined according to recent research (Table 1).[19–24] Models were meshed with between 21,407 and 29,568 nodes, between 11,206 and 15,658 10-node-quadratic tetrahedron body elements, and between 5129 and 7371 contact elements in the model with the highest and the lowest amounts of bone loss, respectively (Fig. 2). As to boundary conditions, all nodes at the bottom of the model were restrained so that rigid body motion was prevented.

The study was divided into three parts. In part 1, three models without splinted crowns (with normal, and 4 mm and 8 mm of bone loss) were loaded with a 25-N force vector on each premolar to assess the stress situation of the alveolar crest compared to apical stress to show that the crestal stress was greater than apical ones in loading separate (non-splint) crowns.

In part 2, 10 models with splinted crowns and gradual bone loss were loaded with a vertical force

Table 1. Material properties used in the finite element models

Material	Young's modulus (kg/cm^2)	Poisson's ratio
Enamel	8.26×10^5	0.33
Dentin	2.14×10^5	0.31
Periodontal ligament	70.3	0.49
Spongy bone	2.15×10^3	0.38
Cortical bone	1.45×10^5	0.26

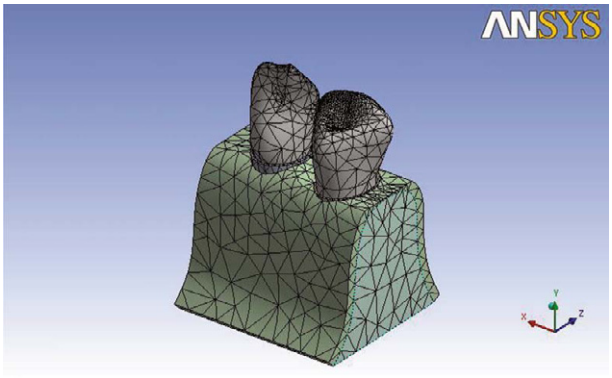

Fig. 2 Meshed model with 1 mm of alveolar bone loss in the second premolar.

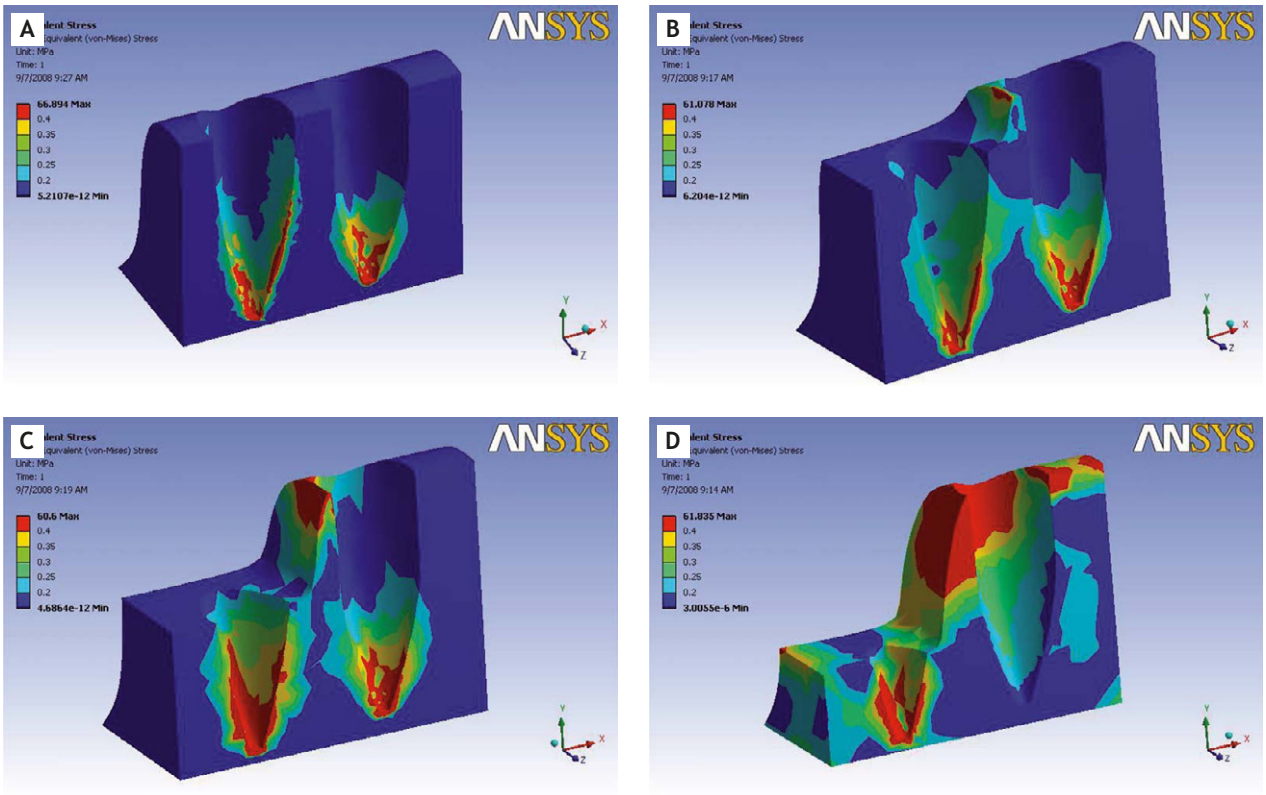

Fig. 3 von Mises stress distributions in splinted models: (A) with 1 mm of alveolar bone loss, (B) with 3 mm of alveolar bone loss, (C) with 7 mm of alveolar bone loss, and (D) with 9 mm of alveolar bone loss.

vector of 25 N onto each premolar crown. This stage was intended to determine the desired C/R ratio beyond which splinting was of little use.

In part 3, three splinted crown models with 1 mm, 4 mm, and 8 mm of bone loss were loaded with a non-axial load of 25 N directed 15° towards the mesial to evaluate the effects of non-axial loads.

Application of a vertical force of 25 N at each occlusal surface of the premolars was based on previous studies.[10,11] von Mises stresses were evaluated in three locations in the bone for all models: the apical area of the first premolar, the apical area of the second premolar, and the alveolar crest between premolars midway buccolingually reached trough slicing the models.

Results

Results are divided according to the stages of this study. Loading non-splinted crowns revealed a higher stress in the alveolar crest area than in the apical area of the premolar (Table 2). In the apical area of the first premolar, the von Mises stresses in this area were in a range of 1.4–2.2 MPa in different alveolar bone loss models with no predictable pattern in gradual bone loss. In the apical area of the second premolar, the findings in this area were 1.477 MPa for the healthy model, which increased to 2.099 MPa in the model with 8 mm of bone loss. In the alveolar crest area, the findings began at 0.141 MPa for the healthy model and increased to 3.405 MPa in the model with 8 mm of bone loss. These findings showed a predictable increase with the progression of bone loss.

Table 2. von Mises stress findings in non-splint models

	Stress (MPa)		
	AP5	Crest	AP4
Normal	1.477	0.141	1.990
With 4 mm of bone loss	1.559	2.129	1.405
With 8 mm of bone loss	2.099	3.405	2.253

AP5 = apical area of the second premolar; Crest = intercrestal area between the premolars; AP4 = apical area of the first premolar.

In the loaded splinted crown models with gradual bone loss, some stress modifications at the three points of assessment were revealed (Fig. 3), and numeric data of von Mises stresses in the different models are given in Table 3. In the apical area of

Table 3. von Mises stress in each model assessed in the bone socket of the teeth in three different locations midway mediolaterally

C/R ratio	Stress (MPa)		
	AP5	Crest	AP4
0.67	1.495	0.144	2.063
0.80	1.296	0.271	1.955
0.95	1.607	0.443	2.008
1.14	1.531	0.854	2.059
1.37	1.789	0.861	1.685
1.65	1.832	1.602	2.049
2.00	1.830	1.583	2.163
2.46	1.974	2.010	1.775
3.09	3.170	2.083	1.883

C/R=crown to root; AP5=apical area of the second premolar; Crest=intercrestal area between the premolars; AP4= apical area of the first premolar.

Table 4. Stress findings in non-axial loading (15° shift in the vertical)

	Stress (MPa)		
	AP5	Crest	AP4
With 1 mm of bone loss	1.364	0.297	2.888
With 4 mm of bone loss	1.848	0.922	2.813
With 8 mm of bone loss	2.865	0.613	2.907

AP5=apical area of the second premolar; Crest=intercrestal area between the premolars; AP4=apical area of the first premolar.

the first premolar, the findings of the von Mises stresses in this area were around 2 MPa in all phases of alveolar bone loss. These findings did not show a clear pattern of changes in different bone loss models. It could be considered to be the same in the various models. In the apical area of the second premolar, the findings were 1.495 MPa for the model with 1 mm of bone loss, which increased to 3.170 MPa in the model with a C/R ratio of 3.09. The pattern clearly showed an increase in stress with a gradual loss of alveolar bone. The increase in stress reached twofold. In the alveolar crest area, the findings began at 0.144 MPa for the 1-mm bone loss model and increased to 2.083 MPa in the last phase of the study in the model with a C/R ratio of 3.09, which was about a 14.5-fold increase.

With application of non-axial loads in the three splinted crown models with 1 mm, 4 mm, and 8 mm of bone loss, the efficiency of splinting with non-axial loads was revealed (Table 4). In the apical area of the first premolar, the von Mises stresses were 2.81–2.90 MPa in all phases of alveolar bone loss without showing a clear pattern of changes in the different bone loss models. In the apical area of the second premolar, the findings were 1.364 MPa for the model with 1 mm of bone loss, which increased to 2.865 MPa in the model with 8 mm of bone loss. The pattern was clearly an increase in this stress with gradual loss of alveolar bone. In the alveolar crest area, findings began at 0.297 MPa for the 1-mm bone loss model and increased to 0.922 MPa in the last phase of the study in the model with 4 mm of bone loss.

Discussion

Favorable masticatory forces within a healthy periodontium, which thereby avoid occlusal trauma, are a primary concern in partially edentulous restorations. Ante's law,[14] Ewing's requirements,[9] and cross-arch stabilization[26,27] are all clinical guidelines used to address this fundamental problem. Teeth may have a less-than-ideal prognosis as abutments for an RPD when there is slight mobility or an unfavorable C/R ratio, perhaps combined with a conical root.[1]

The present study, as well as previous investigation,[9] demonstrated the preferential development of stresses within osseous defects and their variations with the amount of periodontal support. These stress concentrations suggest that occlusal forces can exacerbate the situation in the defect region and possibly cause further bone resorption, depending on their magnitude and frequency. Loss of bone support increases the maximum stresses generated in the supporting structures, especially in the alveolar bone crest. After horizontal bone loss from periodontal disease, the PDL-supported root surface area can be dramatically reduced. In addition, bending moments affecting the supporting bone may be magnified because of the greater leverage associated with a lengthened clinical crown. That may explain the increased deflection and stress generated in models with low bone support.[28]

A splint, according to the *Glossary of Periodontic Terms* is "an appliance designed to stabilize mobile teeth".[3] There is general agreement to splint bilateral distal extension cases to their healthy adjacent teeth when the terminal abutments have reduced support or unfavorable root forms.

The improvement in stress distribution to the supporting structures with fixed splinting was demonstrated for both mandibular and maxillary RPDs with various attachment retainers.[3,13,29] The results of our study with respect to the effect of fixed splinting are in agreement with previous articles[3,13,29] However, there were some differences in the maximum stresses and their distributions observed within the periodontal structures after fixed splinting.

The findings of the present investigation indicated that fixed splinting of periodontally compromised teeth can reduce the stress in the interdental crest area compared to the loading of non-splinted crown models, which can protect this weak area against destructive stresses. Indeed, fixed splinting improves the stress distribution in the surrounding bone and transfers stress from the interdental crest to the apical area of teeth where there is better resistance. Another point worth mentioning in this part of the study was the von Mises stress findings of the crestal bone in the healthy tooth structure model. This stress was lower than the apical stress of both premolars. This prevents us from splinting healthy teeth for retention after orthodontic treatment.

The efficiency of splinting in non-axial loading was also shown in this study (Table 4). Although fixed splinting is a time-honored method of improving the status of weak abutments, there are certain precautions that should not be overlooked. It is seldom beneficial to splint an extremely weak abutting tooth to a strong one. The result is generally to weaken the strong abutment rather than strengthening the weak abutment.[28,30] Phoenix et al.[1] believed that sometimes it is advantageous to sacrifice a periodontally compromised tooth if an adjacent tooth can serve as a better abutment.

Previous studies reported that the lifespan of RPD abutments greatly depends on the quality of periodontal support rather than its quantity.[31,32] It was demonstrated that teeth with bone loss may successfully be used as RPD abutments if splinted properly, and their long-term maintenance is ensured.[33,34]

Kratochvil and Caputo[35] showed that physiologic adjustment has a great influence on the direction of force exerted on the abutments, PDL, and bone supporting a distal-extension RPD. An unadjusted casting exerts a tipping and torque action on the teeth and periodontium. Previous photoelastic and finite element stress analyses showed that an adjusted RPD has a favorably altered stress distribution in the periodontium with severe supporting bone loss.[2,5,36–39]

Nyman and Lindhe[16] showed that under normal circumstances, a C/R ratio of 1:1 is considered the minimum ratio that is acceptable for a FPD abutment. Itoh et al.[3] believed that positive effects of fixed splinting of RPD abutments are more pronounced as the severity of the periodontal defect increases. A review of RPD therapy by Phoenix et al.[1] pointed out that a tooth that has lost more than 50% of its bone support is a poor candidate for fixed splinting. In contrast, the findings of our study suggest that by fixed splinting of a weak abutment even with a C/R ratio of 1.65–2 to its adjacent tooth, the stress distribution is improved to produce a lower stress in the crestal bone compared to the apical regions (Fig. 4). But with higher C/R ratios, stresses in the supporting structures significantly increase, and this periodontally questionable tooth should be condemned in favor of using an adjacent healthy tooth as the abutment, even though the span is increased by one tooth by doing so.

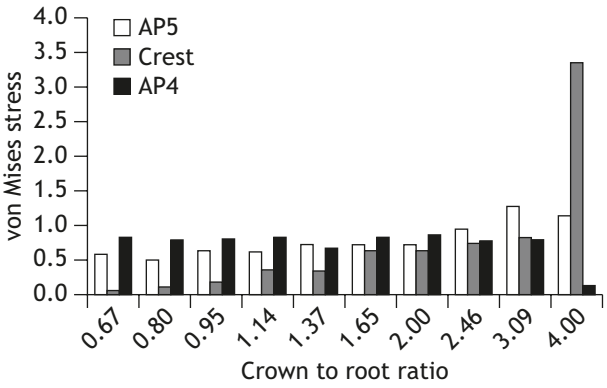

Fig. 4 von Mises stresses in apical areas and crestal bone. AP5=apical area of the second premolar; Crest=intercrestal area between the premolars; AP4=apical area of the first premolar.

To construct a finite element model, it is usually necessary to simplify the system by making some assumptions. The final model represents an average clinical situation, and generalization of its results should be done with care.[40,41] Therefore, because the finite element models used in this study do not identically reproduce all clinical situations, the application of the results should be tempered with sound clinical judgment. However, this study suggests that when an abutment displays decreased periodontal support, fixed splinting may provide adequate support and stabilization for an RPD, but it is not a method of salvaging a tooth with an otherwise hopeless prognosis.

Within the limitations of this 3D finite element stress analysis study, the following conclusions were drawn: (1) splinting a tooth with reduced bone height to an adjacent healthy tooth redirects stress from the bone crest to the apical areas of both teeth; (2) even after fixed splinting of two abutments, gradual loss of bone support increases the stress in the alveolar crest area; (3) fixed splinting of a very weak abutment to an adjacent healthy tooth might not be beneficial (the maximum acceptable C/R ratio for fixed splinting of a weak abutment to adjacent normal tooth was shown to be 1.65–2); and (4) splinted teeth can tolerate non-axial loads.

References

1. Phoenix RD, Cagna DR, Defreest CF. *Stewart's Clinical Removable Partial Prosthodontics*, 4th ed. Chicago: Quintessence Publishing Co, 2008.

2. Carr AB, McGiveny GP, Brown DT. *McCracken's Removable Partial Prosthodontics*, 11th ed. St Louis, MO: Mosby Inc, 2005.
3. Itoh H, Caputo AA, Wylie R, Berg T. Effects of periodontal support and fixed splinting on load transfer by removable partial dentures. *J Prosthet Dent* 1998;79:465–71.
4. Petridis H, Hempton TJ. Periodontal considerations in removable partial denture treatments: a review of literatures. *Int J Prosthodont* 2001;14:164–72.
5. Nogawa A. Study on the dynamic behavior of mandibular distal-extension removable partial denture utilizing finite element method. *Nihon Hotetsu Shika Gakkai Zasshi* 1989; 33:952–65. [In Japanese, English abstract]
6. Lin CL, Chang SH, Wang JC, Chang WJ. Mechanical interactions of an implant/tooth-supported system under different periodontal supports and number of splinted teeth with rigid and non-rigid connections. *J Dent* 2006;34:682–91.
7. Nyman SR, Lang NP. Tooth mobility and the biological rationale for splinting teeth. *Periodontol 2000* 1994;4:15–22.
8. Shillinburg HT, Hobo S, Whitsett LD, Jacobi R, Brackett SE. Treatment planning for the replacement of missing teeth. In: Shillinburg HT, Hobo S, Whitsett LD, Jacobi R, Brackett SE, eds. *Fundamental of Fixed Prosthodontics*, 3rd ed. Chicago: Quintessence Publishing Co, 1997:89–93.
9. Wylie R, Caputo AA. Fixed cantilever splints on teeth with normal and reduced periodontal support. *J Prosthet Dent* 1991;66:734–42.
10. Yang HS, Lang LA, Felton DA. Finite element stress analysis on the effect of splinting in fixed partial dentures. *J Prosthet Dent* 1999;81:721–8.
11. Yang HS, Chung HJ, Park YJ. Stress analysis of a cantilevered fixed partial denture with normal and reduced bone support. *J Prosthet Dent* 1996;76:424–30.
12. Wang CH, Lee HE, Wang CC, Chang HP. Methods to improve a periodontally involved terminal abutment of a cantilever fixed partial denture: a finite element stress analysis. *J Oral Rehabil* 1998;25:253–7.
13. Berg T, Caputo AA. Maxillary distal-extension removable partial denture abutments with reduced periodontal support. *J Prosthet Dent* 1993;70:245–50.
14. Ante IH. The fundamental principles of abutments. *Mich State Dent Soc Bull* 1926;8:14–23.
15. Nyman S, Ericsson I. The capacity of reduced periodontal tissues to support fixed bridgework. *J Clin Periodontol* 1982; 9:409–14.
16. Nyman S, Lindhe J. Prosthetic rehabilitation of patients with advanced periodontal disease. *J Clin Periodontol* 1976;3: 135–47.
17. Aydin AK, Tekkaya AE. Stresses induced by different loadings around weak abutments. *J Prosthet Dent* 1992;68:879–84.
18. Korioth TW, Versluis A. Modeling the mechanical behavior of the jaws and their related structures by finite element (FE) analysis. *Crit Rev Oral Biol Med* 1997;8:90–104.
19. Geramy A. Alveolar bone resorption and the center of resistance modification (3D analysis by means of the finite element method). *Am J Orthod Dentofacial Orthop* 2000; 117:399–405.
20. Geramy A. Initial stress produced in the periodontal membrane by orthodontic loads in the presence of varying loss of alveolar bone: a three-dimensional finite element analysis. *Eur J Orthod* 2002;24:21–33.
21. Geramy A. Optimization of unilateral overjet management: three-dimensional analysis by the finite element method. *Angle Orthod* 2002;72:585–92.
22. Geramy A, Morgano SM. Finite element analysis of three designs of an implant-supported molar crown. *J Prosthet Dent* 2004;92:434–40.
23. Geramy A, Sharafodding F. Abfraction: 3D analysis by means of finite element method. *Quintessence Int* 2003;34: 526–33.
24. Geramy A, Faghihi S. Secondary trauma from occlusion: three-dimensional analysis using the finite element method. *Quintessence Int* 2004;35:835–43.
25. Ash MM, Nelson SJ. The permanent mandibular premolars. In: Ash MM, Nelson SJ, eds. *Wheeler's Dental Anatomy, Physiology and Occlusion*, 7th ed. Philadelphia: WB Saunders Co, 1993: 218–40.
26. Simring M. Splinting: theory and practice. *J Am Dent Assoc* 1952;45:402–14.
27. Ward H, Weinberg L. An evaluation of periodontal splinting. *J Am Dent Assoc* 1961;63:48–54.
28. Wei M, Wang M, Lin YH, Luo Y. Stress distribution on periodontium of separated removable partial denture assembly. *Hua Xi Kou Qiang Yi Xue Za Zhi* 2008;26:387–90, 395. [In Chinese, English abstract]
29. el Charkawi HG, el Wakad MT. Effect of splinting on load distribution of extracoronal attachment with distal extension prosthesis in vitro. *J Prosthet Dent* 1996;76:315–20.
30. Serio FG. Clinical rationale for tooth stabilization and splinting. *Dent Clin North Am* 1999;43:1–6.
31. Nyman S, Lindhe J. A longitudinal study of combined periodontal and prosthetic treatment of patients with advanced periodontal disease. *J Periodontol* 1979;50:163–9.
32. Lundgren D. Prosthetic reconstruction of dentitions seriously compromised by periodontal disease. *J Clin Periodontol* 1991;18:390–5.
33. Brudvik JS, Ma PS. Managing the maxillary partially edentulous patient with extensive anterior tooth loss and advanced periodontal disease using a removable partial denture: a clinical report. *J Prosthet Dent* 2008;100:259–63.
34. Kanno T, Nakamura K, Hayashi E, Kimura K, Hirooka H, Kimura K. What prosthodontic therapy should we select for periodontally compromised patients? Part 2: Review of the literature focusing on conventional prosthodontic therapy for periodontally compromised patients and clinical implication (RPD vs FPD vs implant). *Nihon Hotetsu Shika Gakkai Zasshi* 2008;52:143–9. [In Japanese, English abstract]
35. Kratochvil FJ, Caputo AA. Photoelastic analysis of pressure on teeth and bone supporting removable partial dentures. *J Prosthet Dent* 1974;32:52–61.
36. Inukai M, Baba K, John MT, Igarashi Y. Does removable partial denture quality affect individuals' oral health? *J Dent Res* 2008;87:736–9.
37. Bodineau-Mobarak A, Veille-Finet A, Tenenbaum A. Hygiene and maintenance of removable dental prostheses. *Soins Gerontol* 2008;70:45–6. [In French]
38. Chaiyabutr Y, Brudvik JS. Removable partial denture design using milled abutment surfaces and minimal soft tissue coverage for periodontally compromised teeth: a clinical report. *J Prosthet Dent* 2008;99:263–6.
39. Zlatarić DK, Celebić A, Valentić-Peruzović M. The effect of removable partial dentures on periodontal health of abutment and non-abutment teeth. *J Periodontol* 2002;73: 137–44.
40. Gharechahi J, Sharifi E, Aghdaee NA, Nosohian S. Finite element method analysis of the stress distribution to supporting tissues in a Class IV Aramany removable partial denture (Part I: the teeth and periodontal ligament). *J Contemp Dent Pract* 2008;9:65–72.
41. Gharechahi J, Sharifi E, Nosohian S, Aghdaee NA. Finite element method analysis of stress distribution to supporting tissues in a Class IV Aramany removable partial denture (Part II: bone and mucosal membrane). *J Contemp Dent Pract* 2008;9:49–56.

J Dent Sci 2010;5(1):8–13

ORIGINAL ARTICLE

Effect of 1% chlorhexidine gel on the bonding strength to dentin

Mehmet Dalli,[1] Ertuğrul Ercan,[2] Yahya Orçun Zorba,[3] Bayram İnce,[1] Cafer Şahbaz,[1] Emrullah Bahşi,[1] Hakan Çolak[2]*

[1]Department of Operative Dentistry, Dental School, Dicle University, Diyarbakir, Turkey
[2]Department of Operative Dentistry, Dental School, Kirikkale University, Kirikkale, Turkey
[3]Department of Operative Dentistry, Dental School, Erciyes University, Kayseri, Turkey

Received: Oct 13, 2009
Accepted: Jan 10, 2010

KEY WORDS:
adhesion;
bond strength;
cavity disinfection;
chlorhexidine gel;
posterior composite resin

Background/purpose: The purpose of this *in vitro* study was to evaluate the effect of 1% chlorhexidine (CHX) gel on dentin bond strengths of posterior composite resin applied with two different adhesive systems.
Material and methods: In total, 75 extracted, caries-free human molars were used. The occlusal surface of each tooth was ground to create a flat dentin surface. Then, each tooth was mounted in acrylic. The dentin specimens were randomly assigned to five groups of 15 specimens each. In Group 1, Prime & Bond NT (PBNT) was applied; in Group 2, a 1% CHX gel+etching for 15 s+PBNT were applied; in Group 3, etching+1% CHX gel+PBNT were applied; in Group 4, Clearfil S^3 Bond was applied; and in Group 5, 1% CHX gel+Clearfil S^3 Bond were applied. A dentine bonding system was applied to dentin surfaces, and composite cylinders were built up using a special device and then light-polymerized. Specimens were mounted and sheared using an Instron universal testing machine at a cross-head speed of 0.5 mm/min.
Results: The results were recorded in megapascals. The sheared specimens were examined under a light microscope, and the type of failure (adhesive, cohesive or mixed) was recorded. Data were compared by one-way analysis of variance and Tukey's honestly significant difference tests. Means were 16.4±4.1 MPa in Group 1, 16.2±3.9 MPa in Group 2, 13.0±4.5 MPa in Group 3, 11.9±2.7 MPa in Group 4, and 11.5±2.7 MPa in Group 5. The use of 1% CHX gel before acid etching was significantly higher than after etching on the shear bond strength of PBNT ($P<0.05$), but did not differ significantly from PBNT alone ($P>0.05$).
Conclusion: Within the limitations of the present *in vitro* study, it was concluded that 1% CHX gel application did not adversely affect the shear bond strengths of dentin-bonding agents.

Introduction

In response to increasing esthetic demands of patients, the use of composite resin materials for posterior tooth restorations is increasing.[1] This increase is due primarily to demands for improved esthetics. However, it is generally accepted that resin composites are not yet able to guarantee excellent results when used for posterior tooth restorations. This is due to postoperative sensitivity and penetration of

*Corresponding author. Department of Operative Dentistry, Dental School, Dicle University, Diyarbakir 21230, Turkey.
E-mail: mdalli@dicle.edu.tr

microorganisms and/or their toxic products that, in turn, can cause pulpal lesions and secondary caries.[2]

Bacterially contaminated cavity walls associated with caries are a potential problem in restorative dentistry.[3] Bacteria can remain in the smear layer or in dentinal tubules, and can potentially multiply.[4] Studies indicate that residual bacteria might proliferate from the smear layer beneath restorations, allowing toxins to diffuse to the pulp, resulting in irritation and inflammation.[3,4] It was argued that microorganisms that are present in the cavity walls cannot be removed by the use of water spray or by the effect of restorative materials containing disinfecting agents.[5] Therefore, the adjunctive use of antibacterial solutions after cavity preparation may be considered a method to reduce the incidence of postoperative sensitivity by eliminating viable bacteria and their toxins from the restorative interface.[6] The use of a cavity disinfectant before applying a dentin adhesive agent can reduce or eliminate postoperative sensitivity in composite restorations.[3]

Researchers have applied various alternative approaches to eliminate residual bacteria left in cavity preparations. Treatments with a disinfectant wash and different antibacterial agents have been tested.[4,5] Commercially available disinfectants containing compounds such as chlorhexidine (CHX) digluconate, disodium ethylenediaminetetraacetic acid (EDTA) dihydrate, sodium hypochlorite, hydrogen peroxide, and iodine are used to remove bacterial contaminants.[7,8] Of these, CHX is commonly used to remove bacterial contaminants. CHX is an effective agent for disinfecting dentin. Silva et al.[9] reported a significant decrease in the number of bacteria in dentinal tubules after application of 0.2% CHX for 5 minutes. It is also effective in reducing the levels of *Streptococcus mutans* found on exposed carious root surfaces.[10]

CHX has a strong suppressive effect on *S. mutans* and *S. sobrinus*.[3,11] These microorganisms are of major importance in the development of initial caries.[4] The use of a CHX cavity cleanser after tooth preparation can reduce residual caries and postoperative sensitivity.[3,12,13]

CHX is widely used as an antimicrobial agent and for disinfection before placement of restorations.[7] A CHX solution is active against a wide range of microorganisms, because it is bacteriostatic at low concentrations and bactericidal at higher concentrations.[13] CHX may also inhibit bacterial adherence to surfaces and to each other by competing with calcium for retention sites and, thus, may prevent the formation of calcium bridges between bacteria and oral surfaces or between bacteria.[12] Therefore, the use of solutions such as CHX, which have an antibacterial or bactericidal effect, provides an adjunct treatment that contributes to the suppression of residual infection, thereby increasing survival of restored teeth.[11] Thus, this study evaluated the effects of CHX gel (before and after acid etching) on the shear bond strength of composites with two bonding systems.

Materials and methods

Seventy-five extracted, intact human molars were chosen for this study. All teeth were hand-scaled; all soft tissue was removed, and the teeth were stored in room-temperature tap water for 1 week prior to bonding. Teeth were sectioned with a low-speed diamond disk saw (IsoMet; Buehler, Lake Bluff, IL, USA) under water coolant to expose the mid-coronal dentin. Sections of the teeth, including the roots, were mounted inside a cylindrical-shaped plastic material, 2.5 cm in diameter and with a height of 5 cm, using autopolymerizing acrylic resin. Dentin surfaces were flattened using 600-, 800-, and 1200-grit waterproof polishing papers to create a standardized dentin surface, and the teeth were randomly divided into five groups of 15 teeth each.

In Group 1, the dentin surface was etched with 34% phosphoric acid gel (Dentsply Caulk, Milford, DE, USA) for 15 seconds, rinsed with water for 20 seconds, and dried with absorbent paper. Then, Prime & Bond NT (PBNT) (Dentsply Caulk, Milford, DE, USA) was applied and left undisturbed for 30 seconds, lightly air-dried for 2 seconds, and light-cured for 20 seconds with a light-emitting diode (LED) (Elipar FreeLight; 3M ESPE AG, Seefeld, Germany). After application of an adhesive, specimens were clamped in an Ultradent bonding jig (Ultradent Products, Inc., South Jordan, UT, USA). A posterior composite (Quixfil; Dentsply DeTrey, Konstanz, Germany) was carefully inserted into the surface by packing the material into cylindrical-shaped plastic matrices with an internal diameter of 2.34 mm and a height of 3 mm. Excess composite was carefully removed from the periphery of the matrix with an explorer. The composite was cured with an LED for 20 seconds.

In Group 2, CHX gel (at 1%; Drogsan Pharmaceuticals, Ankara, Turkey) was applied using a disposable brush tip and left undisturbed for 20 seconds. Next, the dentin surface was etched with 37% phosphoric acid for 15 seconds, rinsed with water for 20 seconds, and dried with absorbent paper. The bonding procedure was the same as that in Group 1.

In Group 3, the dentin surface was etched with 37% phosphoric acid for 15 seconds, rinsed with water for 20 seconds, and dried with absorbent paper. Next, 1% CHX gel was applied using a disposable brush tip, and left undisturbed for 20 seconds. The

application of PBNT and the posterior composite resin was the same as in Group 1.

In Group 4, Clearfil S^3 Bond (Kuraray Medical, Okayama, Japan) was applied and left in place for 20 seconds, dried by blowing high-pressure air over it for 5 seconds, and light-cured for 10 seconds with an LED. After applying the adhesive, specimens were clamped in the Ultradent bonding jig. Posterior composite resin (Clearfil Majesty Posterior Shade A3; Kuraray Medical) was carefully inserted and cured with an LED for 20 s.

In Group 5, 1% CHX gel was applied using a disposable brush tip, and left undisturbed for 20 seconds. Then, Clearfil S^3 Bond was applied and left in place for 20 seconds, dried by blowing high-pressure air over it for 5 seconds, and light-cured for 10 seconds with an LED. Clearfil Majesty Posterior was applied in the same way as in Group 4.

Specimens were stored in distilled water at 37ºC for 24 hours. They were then mounted with the treated surfaces parallel to the shearing rod of an Instron universal testing machine (Instron Corp., Canton, MA, USA) and sheared to failure at a crosshead speed of 0.5 mm/min. The results were recorded in megapascals (MPa). The testing was carried out at room temperature (23ºC) and a relative humidity of 50%.

A one-way analysis of variance was used to detect any significant differences ($P \leq 0.05$) in bond strengths among the groups. *Post hoc* comparisons were made using Tukey's honestly significant difference test. After the test procedure, fractured surfaces were observed with a dissecting microscope (SZ-TP; Olympus, Tokyo, Japan) at a magnification of 20 to determine the failure modes, classified as adhesive failure, cohesive failure within the composite, and cohesive failure within the tooth.

One specimen from each group was randomly selected and sputter-coated with gold after fracture and prepared for scanning electron microscopy (SEM). Coated specimens were then observed under an SEM (JSM-5600; JEOL, Tokyo, Japan) at different magnifications.

Results

Mean shear bond strengths to dentin for the five groups are shown in Table 1. Mean shear bond strength values ranged 11.5–16.4 MPa. In particular, Group 1 (PBNT) showed the highest mean shear bond strength value at 16.4 MPa. No significant differences were found between Groups 1 and 2. The statistical analysis showed that the bond strengths of Group 1 (no CHX gel treatment) were significantly higher than those of Group 3 (CHX gel treatment after etching). In contrast, Group 3 (PBNT) demonstrated a significant decrease in bond strength when 1% CHX gel was applied after acid etching (the statistical differences are given in Table 1).

Groups 1 and 2 demonstrated statistically significant differences with Groups 4 and 5 ($P < 0.01$). When the 1% CHX gel was applied to the dentin surface before Clearfil S^3 Bond (Group 5), the shear bond strength was not affected in this study. No significant differences were found between Groups 4 and 5.

The examination of the debonded samples with a stereomicroscope at 20× magnification showed that the fractures were predominantly adhesive for the agents, as shown in Table 2.

SEM analysis revealed that the dentin surface was covered by a hybrid layer. In all SEM samples, composite resin remnants were found. Fig. 1 shows the dentinal surfaces after applying the shear bond strength test.

Discussion

Recent advances in resin-based adhesives and restorative materials, as well as increased patient demands for esthetic restorations, have increased the use of resin-based composites in posterior teeth. However, secondary caries were found to be the

Table 1. Mean bond strengths (in megapascals) and standard deviations (SDs) of the test groups

Group	*n*	Mean (MPa)	SD
Group 1	15	16.4*	4.1
Group 2	15	16.2*	3.9
Group 3	15	13.0†	4.5
Group 4	15	11.9†‡	2.7
Group 5	15	11.5†‡	2.7

Groups identified with different symbols significantly differ ($P < 0.05$).

Table 2. Failure modes of the test groups*

Group	Failure mode		
	Adhesive	Cohesive	Mixed
Group 1	8	5	2
Group 2	7	5	3
Group 3	7	4	3
Group 4	11	2	2
Group 5	9	5	3

*Although the results of the χ^2 analysis were highly significant ($P < 0.01$), inferences could not be made because of the small sample size and the fact that 75% of cells had an expected count of fewer than 5.

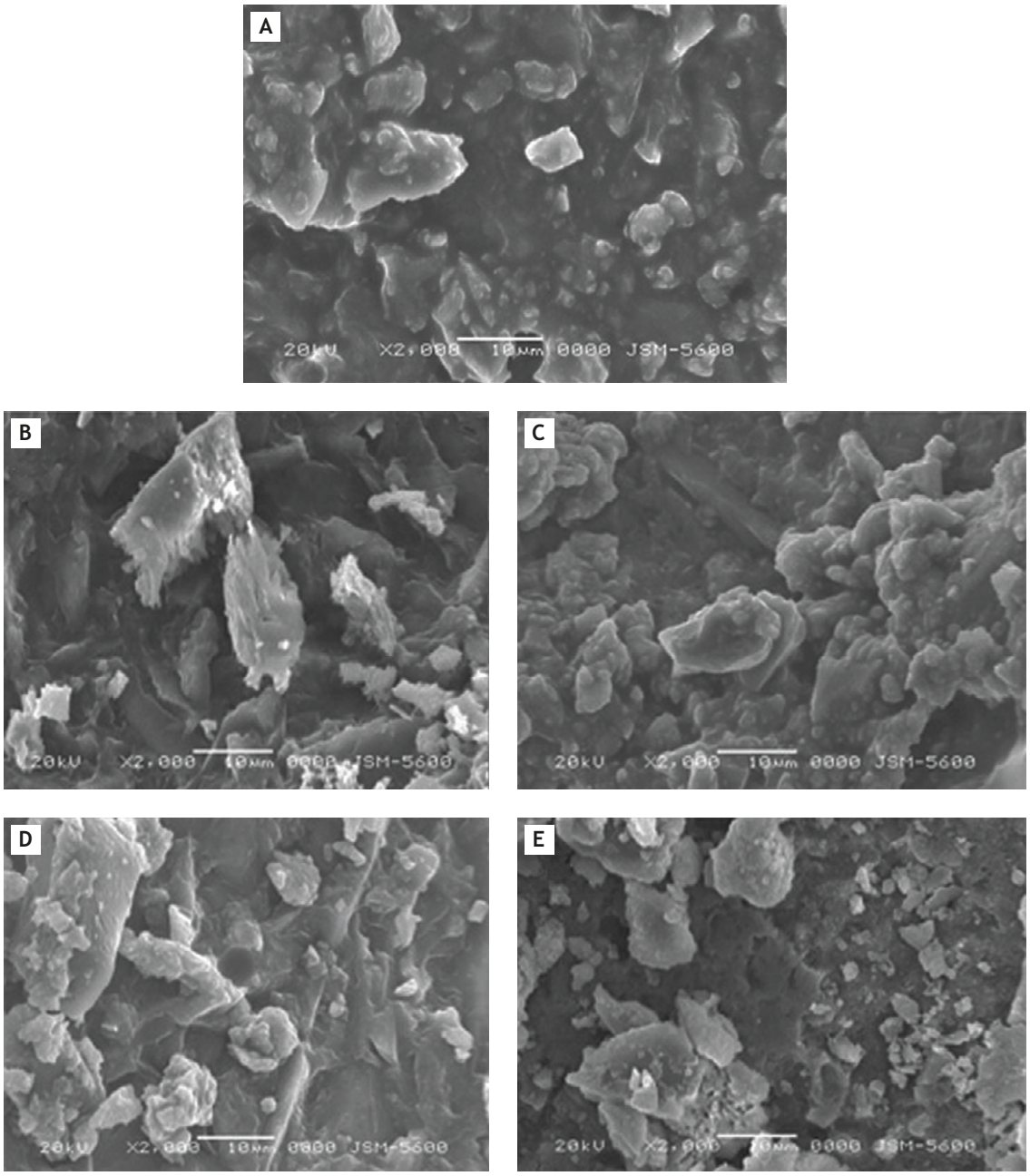

Fig. 1 Scanning electron microscopy photographs of dentin surfaces. (A) Prime & Bond NT was applied; (B) 1% chlorhexidine (CHX) gel was applied before acid etching; (C) 1% CHX gel was applied after acid etching; (D) Clearfil S^3 Bond was applied; (E) Clearfil S^3 Bond was applied after the 1% CHX gel. All images are at the same magnification.

most common reason for replacing resin composite restorations.[14] This may be a result of polymerization shrinkage, which causes a gap between the material and the tooth structure, allowing bacterial penetration.[15] Another source of secondary caries is the presence of bacteria in the smear layer after cavity preparation, which can remain viable for long periods of time.[15] A disinfectant solution, which eliminates these residual bacteria, could be useful after cavity finishing.

One study reported the efficacy of disinfectant solutions.[3] Meiers and Kresin[3] showed that use of CHX products as a cavity cleaner after tooth preparation could reduce the potential for residual caries and postoperative sensitivity. The application of CHX did not negatively affect shear bonding.[16]

The present *in vitro* study showed that CHX gel did not affect the shear bond strength of PBNT before etching the dentin. This result is consistent with recent studies which found that CHX application before and after acid etching did not significantly affect the dentin bonding system.[8,17] In addition, similar studies demonstrated that CHX application prior to acid etching had no adverse

effects on immediate composite adhesive bonds in dentin.[17,18] However, CHX gel adversely affects the shear bond strength of PBNT after etching the dentin. These results correspond to those of Vieira Rde and da Silva,[19] who showed that a cavity disinfectant containing 2% CHX had an adverse effect and produced significantly lower shear bond strengths. In contrast, Gürgan, et al.[20] indicated that application of the CHX before and after acid etching significantly decreased the shear bond strength to dentin. In contrast, those results are inconsistent with the results of Meiers and Shook[4] who found that CHX had no influence on the shear bond strength to dentin.

In vivo and *in vitro* studies by Carrilho et al.[7] and Hebling et al.[21] showed that CHX preserved the hybrid layers with CHX treatment after acid etching.[7,21] The hybrid layer might have decreased the shear bond strength to dentin. The bonding mechanism of the material to the dental structure is another relevant factor. When the smear layer is removed before the restorative material is put in place, the surface's wetting ability is enhanced, leading to the formation of a material tag. Phosphoric acid removes the smear layer, exposes collagen, and reveals the open tubules. The absence of a smear layer after acid treatment produces relatively smooth intertubular dentin without peritubular dentin. Open tubules facilitate the formation of a hybrid or resin-infiltrated layer, creating large surface areas for bonding and allowing the development of resin tags.[22]

Breschi et al.[23] found that the use of CHX as a primer on acid-etched dentin could prevent collagen degradation even after 12 months at a very low concentration (0.2%). In addition, the concentration of CHX did not affect the bond strength. CHX was shown to inhibit the activity of matrix metalloproteinases-2, -8 and -9 through a chelating mechanism, and it also had antibacterial activity.[24] However, it may show a higher antibacterial effect when applied at higher concentrations.[25] In the present study, we applied a 1% gel form of CHX. This form contains a higher concentration of CHX, and it may show longer-lasting adhesion to dentin surfaces than the liquid form of CHX. Further research is needed on adhesion of different CHX forms, between gel and liquid, to dentin surfaces when used to prevent degradation and cavity disinfection.

In the present study, we found that self-etching bonding systems showed lower bond strengths than did etch-and-rinse systems. However, CHX gel application did not affect the shear bond strength. This finding is in agreement with a previous study by Ercan et al.[26] who showed that CHX solution application as a cavity disinfectant decreased the bond strength in self-etching bonding systems. However, the shear bond strength was not adversely affected by CHX solution application when the etch-and-rinse system was used. In addition, CHX gel application had no adverse effect on the shear bond strength of the composite resin. This may have been due to a limited penetration depth of the material in the dentin structure.[26]

In our study, Clearfil S^3 bond did not present any statistically significant difference after CHX gel treatment. This result is in accordance with the study by Soares et al.[17] in which application of a concentration of 0.12% and 2% CHX produced similar behaviors, with no adverse effects on the bond strength. Our results for the shear test showed that bonding with a composite on the dentin was better for teeth treated with PBNT than with Clearfil S^3 Bond. Clearfil S^3 Bond showed the lowest bonding strength on dentin. The differences were statistically significant ($P<0.05$).

Modes of use vary before etching, after etching, rinsing off, or not rinsing. Use of a CHX cleanser before etching was shown not to affect bonding to enamel or dentin.[27] Another study, however, reported reduced dentin bond strengths when a CHX cleanser was used before or after etching, but rinsing the cleanser off before bonding produced bond strengths that were similar to no-cleanser controls.[28] Rinsing away cleansers prior to bonding will most likely prevent undesired material interactions.

The simultaneous etching of enamel and dentin, or total etching techniques, and developments made in chemical adhesives have improved bond strengths.[29] Current developments are focused on simplifying the application of bonding agents by decreasing the time and steps required for placement. As a result, manufacturers have combined the primer and adhesive into a single component but still maintain separate etching and rinsing steps. This method is called two-step bonding.[30]

All dentin surfaces were coated with a hybrid layer; high ratios of composite resin remnants were found on the SEM examination. This may have been due to cohesive or mixed failures of the samples that were selected for SEM examination.

The results from this study indicated that: (1) the shear bond strength was not significantly affected when CHX was applied before etching the dentin surface; (2) there was a significant decrease in bond strength when the 1% CHX gel was applied after acid etching; and (3) when the 1% CHX gel was applied to the dentin surface before Clearfil S^3 Bond, the shear bond strength was not affected.

Within the limitations of this *in vitro* study, the following conclusions were drawn: (1) CHX gel application before phosphoric acid did not influence the shear bond strength of PBNT on dentin, but

CHX gel applied after acid etching had an adverse affect on the shear bonding of PBNT; and (2) the 1% CHX gel had no adverse effect on the bond strength of Clearfil S[3].

References

1. Anderson MH. Current concepts of dental caries and its prevention. *Oper Dent* 2001;26(Suppl 6):11–8.
2. Lopes LG, Cefaly DFG, Franco EB, Mondelli RFL, Lauris JRP, Navarro MFL. Clinical evaluation of two "packable" posterior composite resins two-year results. *Clin Oral Investig* 2003;7:123–8.
3. Meiers JC, Kresin JC. Cavity disinfectants and dentin bonding. *Oper Dent* 1996;12:153–9.
4. Meiers JC, Shook LW. Effect of disinfectants on the bond strength of composite to dentin. *Am J Dent* 1996;9: 11–4.
5. Molgatini S, Abate PF, Negroni MB, Macchi RL, Gonzalez MI. Bacterial inhibition produced by substances for dentin pretreatment. *Acta Odontol Latinoam* 1993;7:3–11.
6. Brannstrom M. The cause of post-restorative sensitivity and its prevention. *J Endod* 1986;12:475–81.
7. Carrilho MR, Carvalho RM, de Goes MF, et al. Chlorhexidine preserves dentin bond in vitro. *J Dent Res* 2007;86:90–4.
8. de Castro FL, de Andrade MF, Duarte Júnior SL, Vaz LG, Ahid FJ. Effect of 2% chlorhexidine on microtensile bond strength of composite to dentin. *J Adhes Dent* 2003;5:129–38.
9. Silva CHFP, Lima KC, Siqueira JF. Dentinal tubule disinfection by chlorhexidine solutions: an in vitro study. *Braz Endod J* 1997;2:55–7.
10. Fure S, Emilson CG. Effect of chlorhexidine gel treatment supplemented with chlorhexidine varnish and resin on mutans streptococci and *Actinomyces* on root surfaces. *Caries Res* 1990;24:242–7.
11. Imazato S, Kuramoto A, Takahashi Y, Ebisu S, Peters MC. In vitro antibacterial effects of the dentin primer of Clearfil Protect Bond. *Dent Mater* 2006;22:527–32.
12. Gjermo P. Chlorhexidine and related compounds. *J Dent Res* 1989;68:1602–8.
13. Matthijs S, Adriaens PA. Chlorhexidine varnishes: a review. *J Clin Periodontol* 2002;29:1–8.
14. Mjor IA, Toffenetti F. Placement and replacement of resin-based composite restorations in Italy. *Oper Dent* 1992;17: 82–5.
15. Brännström M, Vojinovic O. Response of the dental pulp to invasion of bacteria around three filling materials. *J Dent Child* 1976;43:83–9.
16. Filler SJ, Lazarchik DA, Givan DA, Retief DH, Heaven TJ. Shear bond strengths of composite to chlorhexidine-treated enamel. *Am J Dent* 1994;7:85–8.
17. Soares CJ, Pereira CA, Pereira JC, Santana FR, do Prado CJ. Effect of chlorhexidine application on microtensile bond strength to dentin. *Oper Dent* 2008;2:183–8.
18. el-Housseiny AA, Jamjoum H. The effect of caries detector dyes and a cavity cleansing agent on composite resin bonding to enamel and dentin. *J Clin Pediatr Dent* 2000;25:57–63.
19. Vieira Rde S, da Silva IA Jr. Bond strength to primary tooth dentin following disinfection with a chlorhexidine solution: an in vitro study. *Pediatr Dent* 2003;25:49–52.
20. Gürgan S, Bolay S, Kiremitçi A. Effect of disinfectant application methods on the bond strength of composite to dentin. *J Oral Rehabil* 1999;26:836–940.
21. Hebling J, Pashley DH, Tjäderhane L, Tay FR. Chlorhexidine arrests subclinical degradation of dentin hybrid layers in vivo. *J Dent Res* 2005;84:741–6.
22. Pashley DH. Dentin bonding: overview of the substrate with respect to adhesive material. *J Esthet Dent* 1991;3:46–50.
23. Breschi L, Cammelli F, Visintini E, et al. Influence of chlorhexidine concentration on the durability of etch-and-rinse dentin bonds: a 12-month in vitro study. *J Adhes Dent* 2009;11:191–8.
24. Gendron R, Grenier D, Sorsa T, Mayrand D. Inhibition of the activities of matrix metalloproteinases 2, 8, and 9 by chlorhexidine. *Clin Diagn Lab Immunol* 1999;6:437–9.
25. Cousido MC, Tomás Carmona I, García-Caballero L, Limeres J, Alvarez M, Diz P. In vivo substantivity of 0.12% and 0.2% chlorhexidine mouthrinses on salivary bacteria. *Clin Oral Investig* 2009;doi:10.1007/s00784-009-0320-2.
26. Ercan E, Erdemir A, Zobra YO, et al. Effect of different cavity disinfectants on shear bond strength of composite resin to dentin. *J Adhes Dent* 2009;11:343–6.
27. Jarvinen H, Pieniha K, Kinen K, Huovinen P, Tenovuo J. Susceptibility of *Streptococcus mutans* and *Streptococcus sobrinus* to antimicrobial agents after short-term oral chlorhexidine treatment. *J Oral Sci* 1995;103:32–5.
28. Finger WJ, Fritz U. Laboratory evaluation of one component enamel/dentin bonding agents. *Am J Dent* 1996;9:206–10.
29. Gultz J, Do L, Boylan R, Kaim J, Scherer W. Antimicrobial activity of cavity disinfectants *Gen Dent* 1999;47:187–90.
30. Van Meerbeek B, De Munk J, Yoshida Y, et al. Adhesion to enamel and dentin: current status and future challenges. *Oper Dent* 2003;28:215–35.

J Dent Sci 2010;5(1):14–20

ELSEVIER

ORIGINAL ARTICLE

Comparison of the microstructure of crown and root dentin by a scanning electron microscopic study

*Chia-Yi Chu,[1] Tien-Chun Kuo,[2,3] Shu-Fang Chang,[1] Yow-Chyun Shyu,[3] Chun-Pin Lin[2,3]**

[1]Department of Dentistry, Shin Kong Wu Ho-Su Memorial Hospital, Taipei, Taiwan
[2]Graduate Institute of Clinical Dentistry, School of Dentistry, National Taiwan University, Taipei, Taiwan
[3]Department of Dentistry, National Taiwan University Hospital, Taipei, Taiwan

Received: Nov 1, 2009
Accepted: Jan 28, 2010

KEY WORDS:
dentinal tubule;
intertubular dentin;
microstructure of dentin;
root dentin;
scanning electron microscopy

Background/purpose: Detailed information of the dentin microstructure is essential in order to interpret data from investigations on dentin adhesive materials. Most studies of dentin microstructure focused on the crown dentin, and few compared microstructures of the crown and root dentin. The purpose was to compare the density and diameter of dentinal tubules and the thickness of peritubular dentin at the crown, and coronal and middle root.
Materials and methods: Ten caries-free human lower first molars were sectioned into four parts as the chamber roof, chamber wall, coronal root, and middle root. After being immersed in 5.25% NaOCl solution for 30 minutes, sectioned surfaces were examined under a scanning electron microscope. Data of tubule density, diameter, and peritubular dentin thickness in the inner, middle and outer portions were collected. Friedman's nonparametric related sample test and Wilcoxon nonparametric signed rank *post hoc* test were used for data analyses.
Results: Tubule densities of the inner and middle dentin of the root were significantly lower than that of the crown. Peritubular dentin width in the chamber roof was significantly higher than those in other areas of the tooth.
Conclusion: Our findings show that the proportion of the tubular area is lower, and there is less peritubular dentin in the root dentin than in crown dentin. To achieve good bonding of resin to root dentin, it is potentially beneficial to focus on improving the quality of the hybrid layer rather than that of resin tags.

Introduction

Differentiation of odontoblasts during dentinogenesis is the result of an interaction between ectomesenchymal components of the tooth germ.[1] In the crown portion, odontoblasts differentiate from the ectomesenchymal dental papilla and form the first dentin. Cells in the inner dental epithelium then differentiate into ameloblasts and initiate amelogenesis. As a result, a fairly distinct border exists between the enamel and dentin. A similar course occurs in the root. As soon as dentinogenesis begins,

*Corresponding author. Department of Dentistry, National Taiwan University Hospital, 1, Chang-Te Street, Taipei 10048, Taiwan.
E-mail: pinlin@ntu.edu.tw

Hertwig root sheath disintegrates. Cementoblasts then differentiate from the dental sac to form cementum, but the border between the dentin and cementum is indistinct. Despite marked differences in their relations to neighboring tissues, the crown and root dentin are generally considered to be similar or identical.

Studies of dentin structure date back to the early history of light microscopy.[2] A wide range of techniques have been used to reveal its detailed structure, including histochemistry,[3] immunofluorescence microscopy,[4] various types of light microscopy such as polarized,[5] phase-contrast and interference microscopy,[6] microradiography,[7] and transmission[8] and scanning electron microscopy (SEM).[9] But most studies focused on the crown dentin, and relatively few examined structural differences between the crown and root dentin.[10]

Understanding the microstructure of the dentin can provide a basis for improved understanding of the correlation between its structure and properties. Dentin bonding in root canals has become a recent trend in endodontics.[11] However, detailed knowledge about the microstructure of root dentin is still inadequate. Therefore, the purpose of this study was to compare the density and diameter of dentinal tubules and peritubular dentin thickness of the crown and root dentin by SEM as a basis for a dentin adhesion study.

Materials and methods

Ten caries-free human lower first molars, extracted in the dental department of National Taiwan University Hospital due to periodontal reasons from patients at the ages of 34–56 years, were preserved in normal saline at 4°C. Each tooth was split into four specimens with a chisel and hammer, including the chamber roof, the distal aspect of the chamber wall, the distal aspect of the distal root coronal portion, and the distal aspect of the distal root middle portion (Fig. 1). Specimens were thoroughly rinsed with distilled water, and immediately immersed in 5.25% NaOCl for 30 minutes. After several thorough washes with distilled water, they were sequentially dehydrated in an alcoholic series and dried in a desiccator for 24 hours. Specimens were mounted on stubs with the split surface face up, using carbon conductive tapes. Specimens were sputter-coated with gold by vacuum-coating equipment (Bio-Rad SC502; Fisons plc, UK), and examined under a SEM (Topcon ABT-60; Topcon, Tokyo, Japan). Each specimen was divided into inner dentin (within 200 μm from the pulpal surface), middle dentin (between the inner and outer dentin), and outer dentin (within 200 μm of the dentine–cementum junction). The dentin tubule density was calculated under 500× magnification (15 kV; working distance, 15 mm) by counting tubule numbers crossing an imaginary 200-μm line perpendicular to the long axis of the dentinal tubules (Fig. 2). The diameter of the tubules and thickness of the peritubular dentin were observed under 3000× magnification (15 kV; working distance, 15 mm) (Fig. 2). Probability values were computed using Friedman's nonparametric related sample test, and Wilcoxon nonparametric signed rank test with the Bonferroni procedure was used for *post hoc* comparisons.

Results

Fig. 3 shows unprepared pulpal surfaces in four different dentin areas. Treatment with 5.25% NaOCl

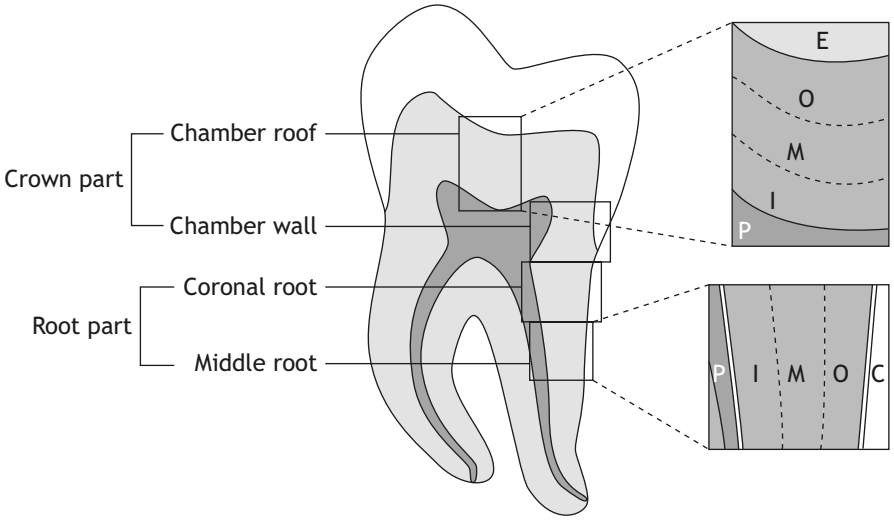

Fig. 1 Diagram of a tooth showing the selected areas to be examined. C=cementum; E=enamel; I=inner dentin; M=middle dentin; O=outer dentin; P=dental pulp.

removed the unmineralized predentin layer revealing the underlying dentinal tubules which were organized into calcospherites. The appearance of the calcospherites in the chamber roof (Fig. 3A) was less apparent compared with other areas.

Fig. 4 demonstrates the split surface of the dentin. Dentinal tubules had heterogeneous densities in different parts. In the inner dentin (Fig. 4A, C, E and G), tubules were highly concentrated in both the crown and root parts, whereas they became

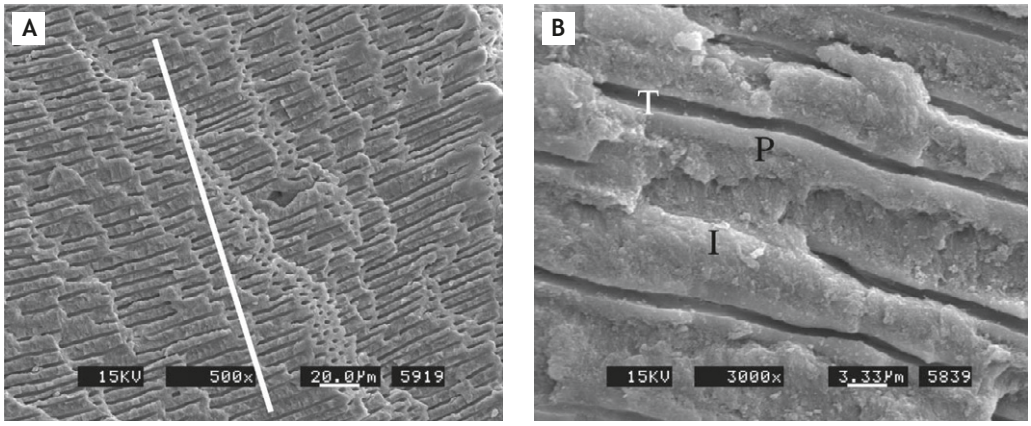

Fig. 2 Scanning electron micrograph illustrating the way to calculate the dentinal tubule density and structures to be examined. (A) Counting tubule number crossing an imaginary 200-μm line (white line) as *N*, then tubule density of this area is $[(N/200)\times 10^3]^2/mm^2$. (B) Structures to be examined. I=intertubular dentin; P=peritubular dentin; T=dentinal tubule.

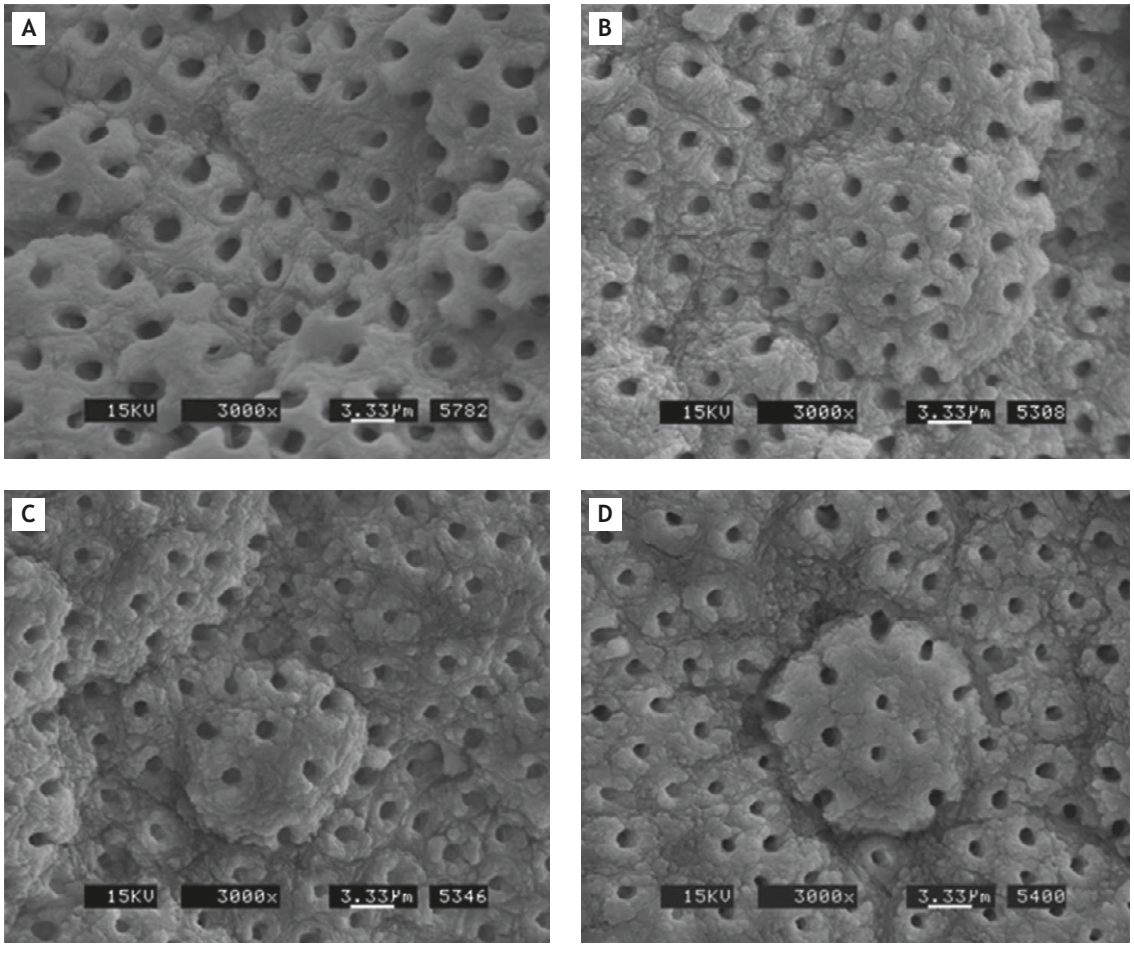

Fig. 3 Unprepared pulpal surfaces of dentin under 3000× scanning electron microscopy examination. (A) Chamber roof; (B) chamber wall; (C) coronal root; (D) middle root. After NaOCl treatment, the predentin was removed to show the underlying mineralized spherical dentin matrix (calcospherites).

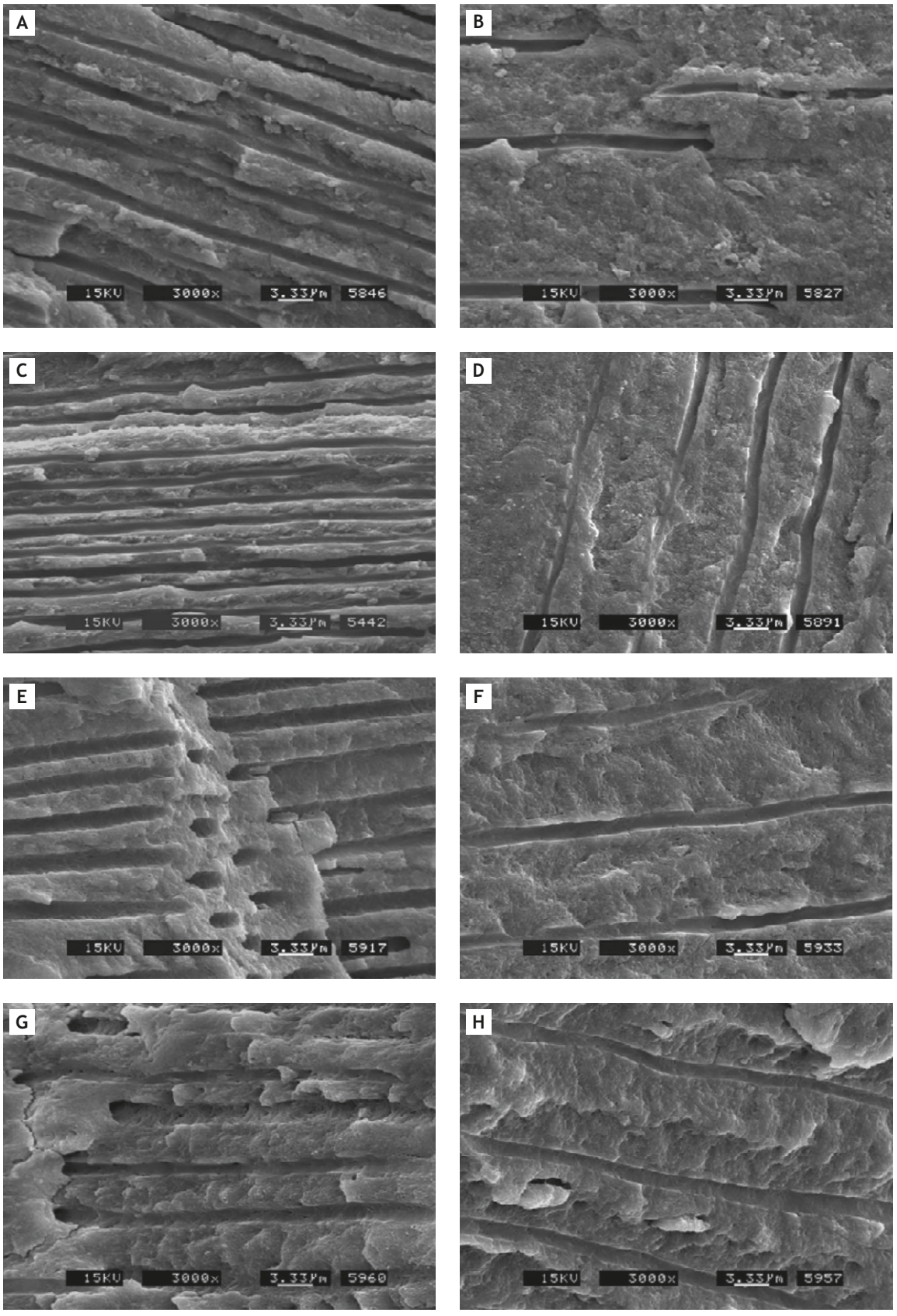

Fig. 4 Split dentin surfaces under 3000× scanning electron microscopy examination. (A) Inner portion of chamber roof; (B) outer portion of chamber roof; (C) inner portion of chamber wall; (D) outer portion of chamber wall; (E) inner portion of coronal root; (F) outer portion of coronal root; (G) inner portion of middle root; (H) outer portion of middle root. The tubular density was significantly higher in the inner dentin (A, C, E and G) than in the outer dentin (B, D, F and H).

much sparser in the outer dentin (Fig. 4B, D, F and H). Compared with the apparent peritubular dentin with its smooth tubule lumen in the crown parts (Fig. 4A–D), the peritubular dentin was indistinct in the root parts (Fig. 4E–H), permitting the reticular fibril nature of the dentin matrix to be seen.

The average diameter and density of the dentinal tubules and the peritubular dentin thickness are shown in Tables 1, 2 and 3. The difference in the density of tubules from the outside inward was more marked in crown parts than in the root. It was significantly greater in the crown part than in the root for the middle and inner dentin (Tables 1 and 4). Tubule diameters of the inner, middle and outer dentin did not show significant differences (Table 2). The peritubular dentin thickness was significantly

Table 1. Density of dentinal tubules ($n=10$)*

	Chamber roof (/mm^2)	Chamber wall (/mm^2)	Coronal root (/mm^2)	Middle root (/mm^2)	P†
Inner dentin	52,900 (49,019–57,600)	66,313 (61,275–70,300)	39,013 (34,731–44,631)	42,050 (36,100–46,769)	<0.001
Middle dentin	34,250 (24,456–39,025)	30,625 (26,575–38,519)	11,563 (8575–15,944)	12,663 (8794–15,944)	<0.001
Outer dentin	7663 (5625–9525)	7250 (5444–12,675)	7250 (6206–9269)	6400 (5625–7225)	0.30

*Data are presented as median (25th–75th percentiles); †probability values were computed by Friedman's nonparametric test for multiple related samples.

Table 2. Average diameter of dentinal tubules ($n=10$)*

	Chamber roof (μm)	Chamber wall (μm)	Coronal root (μm)	Middle root (/mm^2)	P†
Inner dentin	1.90 (1.80–2.23)	1.90 (1.75–2.20)	1.80 (1.65–2.10)	1.80 (1.58–2.23)	0.52
Middle dentin	1.40 (1.20–1.53)	1.45 (1.20–1.53)	1.55 (1.38–1.73)	1.55 (1.28–1.80)	0.42
Outer dentin	0.70 (0.60–1.03)	1.10 (0.80–1.20)	1.00 (0.70–1.28)	1.35 (0.95–1.53)	0.08

*Data are presented as the median (25th–75th percentiles); †probability values were computed by Friedman's nonparametric test for multiple related samples.

Table 3. Average width of peritubular dentin ($n=10$)*

	Chamber roof (μm)	Chamber wall (μm)	Coronal root (μm)	Middle root (/mm^2)	P†
Inner dentin	0.45 (0.08–0.60)	0.00 (0.00–0.25)	0.00 (0.00–0.33)	0.00 (0.00–0.23)	0.01
Middle dentin	0.60 (0.28–1.00)	0.50 (0.15–0.65)	0.20 (0.00–0.50)	0.20 (0.00–0.45)	0.01
Outer dentin	1.20 (0.95–1.45)	0.70 (0.40–1.00)	0.70 (0.55–1.05)	0.40 (0.00–0.85)	0.004

*Data are presented as the median (25th–75th percentiles); †probability values were computed by Friedman's nonparametric test for multiple related samples.

Table 4. Density of dentinal tubules (*post hoc* comparisons)*

	Inner dentin			Middle dentin		
	Chamber roof	Chamber wall	Coronal root	Chamber roof	Chamber wall	Coronal root
Chamber wall	†			NS		
Coronal root	†	†		†	†	
Middle root	†	†	NS	†	†	NS

**Post hoc* multiple comparisons were performed using Wilcoxon nonparametric signed-rank test with the Bonferroni procedure; †P<0.008 indicating a significant difference in the *post hoc* multiple comparisons. NS=not significant.

Table 5. Average width of peritubular dentin (*post hoc* comparisons)*

	Inner dentin			Middle dentin			Outer dentin		
	Chamber roof	Chamber wall	Coronal root	Chamber roof	Chamber wall	Coronal root	Chamber roof	Chamber wall	Coronal root
Chamber wall	†			NS			‡		
Coronal root	NS	NS		†	NS		†	NS	
Middle root	†	NS	NS	NS	NS	NS	‡	NS	NS

**Post hoc* multiple comparisons were performed using Wilcoxon nonparametric signed rank test with the Bonferroni procedure; †$P<0.05$ indicating a significant difference in *post hoc* multiple comparisons without adjusting for the type I error rate; ‡$P<0.008$ indicating a significant difference in the *post hoc* multiple comparisons. NS=not significant.

higher in the chamber roof than in other areas of the tooth (Tables 3 and 5).

Discussion

Estimates of the diameter of tubules, the thickness of the peritubular dentin, and the tubule density were made in a number of studies.[12,13] In our study, the tubule density, diameter, and peritubular dentin thickness of the crown dentin grossly agreed with values reported by previous studies. The tubule densities were about 54,000/mm^2 in the inner dentin, 30,000/mm^2 in the middle dentin, and 8000/mm^2 in the outer dentin. Tubule diameters were about 1.9 μm in the inner dentin, 1.4 μm in the middle dentin, and 1.2 μm in the outer dentin. Bonding to the apical one-third of the root canal is problematic,[11,14] and because of greater variations in this portion, the apical one-third of the root was not included in this study.

The convergence of dentinal tubules from the outer to inner dentin in the root dentin was similar to that in the crown dentin. But differences between the inner and outer dentin were more marked in the crown than in the root. Since both the tubule density and peritubular dentin thickness were greater in the crown than in the root, the proportion of the tubular area in the root dentin was lower, and there was less peritubular dentin lining the root dentin than the crown dentin.

With the rigidity of a root weakened by endodontic and restorative instrumentation,[15,16] the sealing quality and tooth strengthening potential are important issues. To reinforce the roots, the modulus of elasticity of a canal restoration material would need to approximate that of dentin (i.e., 18,000 MPa).[17,18] Restoration of root canal-treated teeth with adhesive restorations offers many advantages over the use of traditional, non-adhesive materials. For instance, bonded resins (with an approximate modulus of elasticity of 16,000–25,000 MPa) permit transmission of functional stresses across the bonded interface to the tooth,[16] with the potential to reinforce a weakened tooth structure.[16,18] When properly using adhesive materials, there is usually no gap between these materials and the tooth structure, greatly reducing microleakage. Application of adhesives to acid-etched dentin creates an acid-resistant, resin-infiltrated collagen layer, the so-called hybrid layer that not only retains composites to dentin, but also can seal dentin from fluids.[19]

Different studies showed marked variations in the reported dentin bond strengths when comparing the crown dentin and root dentin. Some authors reported higher bond strengths to dentin in the root,[20,21] while others reported lower bond strengths.[14,22] These variations might be associated with differences in the size of the prepared surfaces, the presence of a smear layer, the density of tubules, the direction of tubules on the prepared surfaces (i.e., cross-sectioned or longitudinally sectioned or somewhere in between), variations in the intricate branching system, and the presence of highly mineralized peritubular dentin. Thus, testing of the bond strength between a material and a dentin substrate is of limited value if the structure of the dentin sample is not characterized. Detailed information of the dentin microstructure is essential in order to interpret data from investigations on dentin adhesive materials.

Dentin bonding procedures distinctly differ from those of bonding to enamel. Resin tags at the enamel restoration interface improve mechanical bonding; however, this is less important in dentin bonding. The retention of a dentin–resin interface is mostly provided by the hybrid layer formed with the collagen matrix in the intertubular dentin.[23,24] The process of hybridization is believed to result from the infiltration of the primer into the open spatial network in the collagen matrix exposed by dentin demineralization. A slightly moist environment during bonding improves the bond strength, and this procedure has become identified as wet bonding to dentin.[25] Because of the hydrophilic nature of this matrix, we suggest using a hydrophilic bonding

system rather than a hydrophobic bonding system in root canals. Although the bonding surface in root canals has less tubular area for resin tag infiltration, there is more intertubular dentin area with abundant collagen matrix for hybrid layer formation. According to the morphologic characteristics of root dentin observed in our study, it is potentially beneficial to focus on the quality of the hybrid layer to improve resin bonding in the root dentin. Efforts to achieve a stronger resin tag seem to be of less importance.

In addition to structural differences between root dentin and crown dentin, there are other factors, such as an unfavorable geometry, performance difficulties, curing depth, potential interference of adhesive materials with irrigation solutions, and medicaments in root canals, that make bonding of the root canal system a challenge. Further research and material development are mandatory.

References

1. Bath-Balogh M, Fehrenbach MJ. Tooth development and eruption. In: Bath-Balogh M, Fehrenbach MJ, eds. *Illustrated Dental Embryology, Histology, and Anatomy*. Philadelphia: WB Saunders Co, 1997:62–80.
2. Hanazawa K. A study of the minute structures of dentine, especially of the relationship between dentinal tubules and fibrils. *Dent Cosmos* 1917;59:374–405.
3. Symons NBB. A histochemical study of the intertubular and peritubular matrices in normal human dentine. *Arch Oral Biol* 1961;5:241–50.
4. Aubin JE. New immunological approaches to studying the odontoblast. *J Dent Res* 1985;64:515–22.
5. Hals E. Polarized light study of giant tubules in human and red deer coronal dentin. *Scand J Dent Res* 1983;91:105–11.
6. Kaye H, Herold RC. Structure of human dentin, I: phase contrast, polarization, interference and bright field microscopic observations on the lateral branch system. *Arch Oral Biol* 1966;11:355–68.
7. Mjör IA, Shackleford JM. Microradiography of human pulp tissue and decalcified coronal dentine. *Arch Oral Biol* 1966; 11:1307–16.
8. Schroeder L, Frank RM. High-resolution transmission electron microscopy of adult human peritubular dentine. *Cell Tissue Res* 1985;242:449–51.
9. Tronstad L. Ultrastructural observations on human coronal dentin. *Scand J Dent Res* 1973;81:101–11.
10. Mjör IA, Nordahl I. The density and branching of dental tubules in human teeth. *Arch Oral Biol* 1996;41:401–12.
11. Schwartz RS. Adhesive dentistry and endodontics, part 2: bonding in the root canal system-the problems: a review. *J Endod* 2006;32:1125–34.
12. Fosse G, Saele PK, Eide R. Numerical density and distributional pattern of dentin tubules. *Acta Odontol Scand* 1992; 50:201–10.
13. Garberoglio R, Brännström M. Scanning electron microscopic investigation of human dentinal tubules. *Arch Oral Biol* 1976; 21:355–62.
14. Bouillaguet S, Troesch S, Wataha JC, Krejci I, Meyer JM, Pashley DH. Microtensile bond strength between adhesive cements and root canal dentin. *Dent Mater* 2003;19: 199–205.
15. Reeh ES, Messer HH, Douglas WH. Reduction in tooth stiffness as a result of endodontic and restorative procedures. *J Endod* 1989;15:512–6.
16. Lang H, Korkmaz Y, Schneider K, Raab WH. Impact of endodontic treatments on the rigidity of the root. *J Dent Res* 2006;85:364–8.
17. Barjau-Escribano A, Sancho-Bru JL, Forner-Navarro L, Rodrìguez-Cervantes PJ, Pérez-González A, Sánchez-Marín FT. Influence of prefabricated post material on restored teeth: fracture strength and stress distribution. *Oper Dent* 2006;31:47–54.
18. Wu X, Chan ATT, Chen YM, Yip KHK, Smales RJ. Effectiveness and dentin bond strengths of two materials for reinforcing thin-walled roots. *Dent Mater* 2007;23:479–85.
19. Nakabayashi N, Kojima K, Masuhara E. The promotion of adhesion by the infiltration of monomers into tooth substrate. *J Biomed Mater Res* 1982;16:265–73.
20. Gaston BA, West LA, Liewehr FR, Fernandes C, Pashley DH. Evaluation of regional bond strength of resin cement to endodontic surfaces. *J Endod* 2001;27:321–4.
21. Muniz L, Mathias P. The influence of sodium hypochlorite and root canal sealers on post retention in different dentin regions. *Oper Dent* 2005;30:533–9.
22. Yoshiyama M, Matsuo T, Ebisu S, Pashley D. Regional bond strengths of self-etching/self-priming adhesive systems. *J Dent* 1998;26:609–16.
23. Gwinnett AJ. Quantitative contribution of resin infiltration/ hybridization to dentin bonding. *Am J Dent* 1993;6:7–9.
24. Yoshida Y, Nagakane K, Fukuda R, et al. Comparative study on adhesive performance of functional monomers. *J Dent Res* 2004;83:454–8.
25. Kanca JA. Improving bond strength through acid etching of dentin and bonding to wet dentin surfaces. *J Am Dent Assoc* 1992;123:35–43.

J Dent Sci 2010;5(1):21–29

ELSEVIER

ORIGINAL ARTICLE

Evaluation of ten extra-alveolar temporary anchorage device insertion sites by cone beam volumetric computer tomography: a pilot study

Yi-Jyun Chen,[1,2] *Chia-Tze Kao,*[2,3] *Tsui-Hsien Huang*[1,2,3]*

[1]College of Oral Medicine, Chung Shan Medical University, Taichung, Taiwan
[2]Department of Orthodontics, Chung Shan Medical University Hospital, Taichung, Taiwan
[3]Institute of Oral Biology and Biomaterial Science, College of Oral Medicine, Chung Shan Medical University, Taichung, Taiwan

Received: Dec 5, 2009
Accepted: Feb 3, 2010

KEY WORDS:
cone beam volumetric computed tomography;
insertion site;
temporary anchorage device

Background/purpose: In order to increase the success rate of temporary anchorage devices (TADs), it is important not to cause root injury or soft-tissue inflammation. The aim of the present study was to evaluate hard- and soft-tissue thicknesses of TAD insertion sites and the perforation ratio with different lengths of TADs by cone beam volumetric computed tomography (CBCT).
Materials and methods: The hard- and soft-tissue thicknesses were evaluated on 10 patients (5 males and 5 females) by CBCT. The ages ranged 20–36 years. Ten regions of interest (ROIs) in extra-alveolar bone were selected and based on anchorage requirements. Soft-tissue depths were measured in the premaxillary and midpalatal regions, while the cortical bone thicknesses were measured in all the other sites. Data were collected and the Wilcoxon rank sum test was used to compare differences, while the Wilcoxon signed rank test was used for paired data.
Results: The average bone depth of the jaw was around 10 mm at most of the extra-alveolar ROIs, except for the infrazygomatic crest and midpalatal region. The average cortical bone thickness of the jaw was around 2 mm. The soft-tissue depth in the premaxillary region was thicker than that of the midpalatal region ($P<0.05$). The infrazygomatic crest possessed the largest variation of hard-tissue depth. The cortical bone thickness increased from the mesial to the distal in both the buccal and lingual areas of the mandible.
Conclusion: CBCT provides better radiographic evaluation than traditional radiographs. TAD insertion at these 10 extra-alveolar sites introduced in the study could be ideal locations. The design of TADs for different ROIs should take hard- and soft-tissue thicknesses into consideration to reduce clinical complications.

Introduction

Since implants are popularly applied as orthodontic anchorage devices,[1–3] miniscrews are applied in various locations in alveolar bone.[4–7] Compared with dental implants and microplates, miniscrews are smaller in size, cheaper, and easier to insert and remove.[8,9] Although there are many benefits of using miniscrews instead of other temporary anchorage devices (TADs), anatomic sites for safe

*Corresponding author. Institute of Oral Biology and Biomaterial Science, College of Oral Medicine, Chung Shan Medical University, 110, Chien-Kuo North Road, Section 1, Taichung 40201, Taiwan.
E-mail: thh@csmu.edu.tw

insertion are still being discussed in recent years.[10–13]

Because of the risk of injuring the root while inserting a miniscrew in the dental alveolar area, many kinds of the insertion guides that are recorded on radiographs were developed.[14–20] Among all of those techniques, some require computed tomography (CT),[21,22] which entails a relatively high cost and increased radiation exposure.[20,23–27]

Recent studies established CT as a useful technology to evaluate intraoral hard tissues and the best location for implant placement.[10,11,13,21,22,28] Advantages of three-dimensional (3D) imaging are numerous.[29] Studies showed that radiation exposure is much lower for cone beam CT (CBCT) than for medical CT, and closer to the range of standard dental film series.[30,31] Presently, although the existing orthodontic patient data were primarily based on two-dimensional (2D) imaging records, CBCT has led to a multitude of clinical applications across all dental disciplines. CBCT data allow measurement of any area in the scanned volume with increased accuracy and without the projection or superimposition errors of 2D techniques; therefore, 3D imaging can provide more-extensive and more-detailed patient evaluations.[32]

Since the inter-alveolar spaces increase in mesiodistal width from the cementoenamel junction to the apical region,[11,33,34] some studies suggested only placing TADs in apical regions, rather than in the cervical region, to decrease the risk of encountering tooth roots.[20,35] However, the best way to prevent root injury is not to insert a miniscrew in the interradicular area, which means the intra-alveolar area.[13]

Extra-alveolar sites for TADs are strongly recommended when considering the risks of encountering tooth roots.[20,33] In addition, TADs in these areas can provide easier and wider applications in tooth movement, such as posterior segment intrusion,[36,37] anterior teeth retraction,[37] impacted second molar uprighting,[38] maxillary molar distal movement,[28,39] and mandibular molar distal movement.[40] TADs in the inter-radicular area can sometimes impede tooth movement, when a tooth has not moved a sufficient distance to an ideal position and is already touching the TAD, a situation that could never occur if the TAD were placed in the extra-alveolar region.

Hard-tissue quality and quantity affect the success rates of TADs.[41] With thin cortical bone and low-density trabecular bone, TAD insertion loading strain values may exceed the level of microfractures, thus leading to screw loosening.[42] Several studies evaluated the cortical bone thickness at various interradicular areas.[10–12,43,44] However, few reports evaluated hard-tissue thicknesses of extra-alveolar areas.[13,45,46]

With CBCT images, we evaluated extra-alveolar sites for TADs. The aim of this study was to evaluate extra-alveolar TAD insertion sites by CBCT. Ten extra-alveolar regions of interest (ROIs) were chosen based on clinical anchorage requirements, with particular emphasis on measuring the cortical bone thickness and acquired bone depth. The perforation ratios with different lengths of TADs were also calculated.

Materials and methods

The craniofacial morphology of 10 adult Taiwanese (5 women and 5 men, with a mean age of 28.7 ± 5.21 years) with no craniofacial anomalies or trauma or systemic diseases was selected from a CBCT (i-CAT imaging system; Imaging Sciences International, Hatfield, PA, USA) databank. The CBCT settings were 120 kVp and a constant-potential voltage waveshape of 3–8 mA. The source-to-sensor distance was 27 inches (68.5 cm) with scan time of 40 seconds and single 360° rotation for image acquisition. The primary reconstruction was 2 minutes, and voxel size was 0.4–0.2 mm. Multi-planar reformatting of those obtained data and ROI measuring were performed with the i-CAT imaging system.

Images of specific regions were simultaneously displayed with their panoramic, axial and sagittal slices so that each specific ROI could be accurately located (Fig. 1). The images were respectively adjusted to the exact tissue threshold of different ROIs. By adjusting the image size, brightness and contrast with i-CAT Vision (Imaging Sciences International), the hard- and soft-tissue margins were definitively marked as shown in Fig. 2.

Ten extra-alveolar ROIs, chosen for the study of hard and soft tissues, were determined by the versatility of clinical use.[13,28,36–40,47] The terminologies for the anatomic ROIs below were based on standard definitions but modified to narrow the ROI for clarity.[13,47] Furthermore, these ROIs were divided into single and dual sites. Single sites, which were located in the anatomic sagittal plane, included the incisive fossa, premaxillary region, midpalatal region, and symphysis. Dual sites, which were located symmetrically on both sides of the coronal plane, included the canine fossa, infrazygomatic (IZ) crest, anterior external oblique ridge (AEOR), retromolar area, and sublingual fossa.

Anatomic ROIs

Maxilla (3 facial and 2 palatal)

The incisive fossa is limited distally by the canine eminence, inferiorly by the apices of the incisors, and superiorly by the nasal cavity (Figs. 2A and 3A).

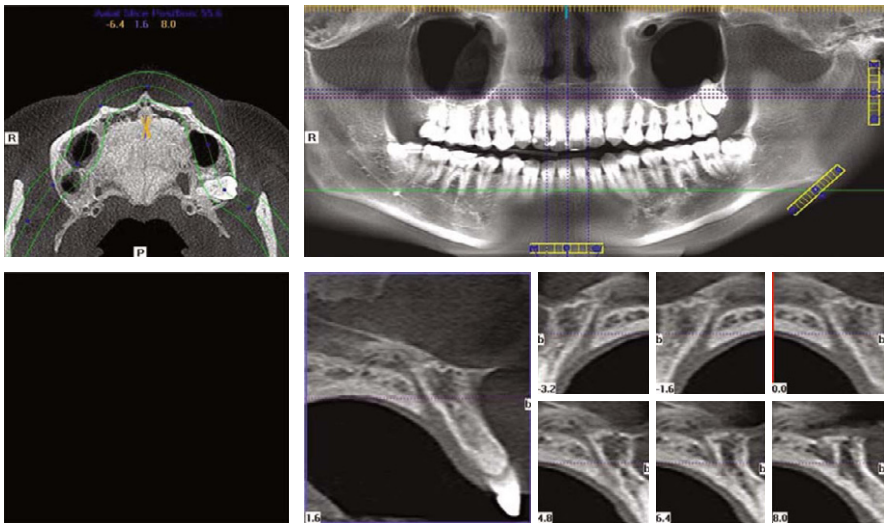

Fig. 1 Specific regions accurately located by software.

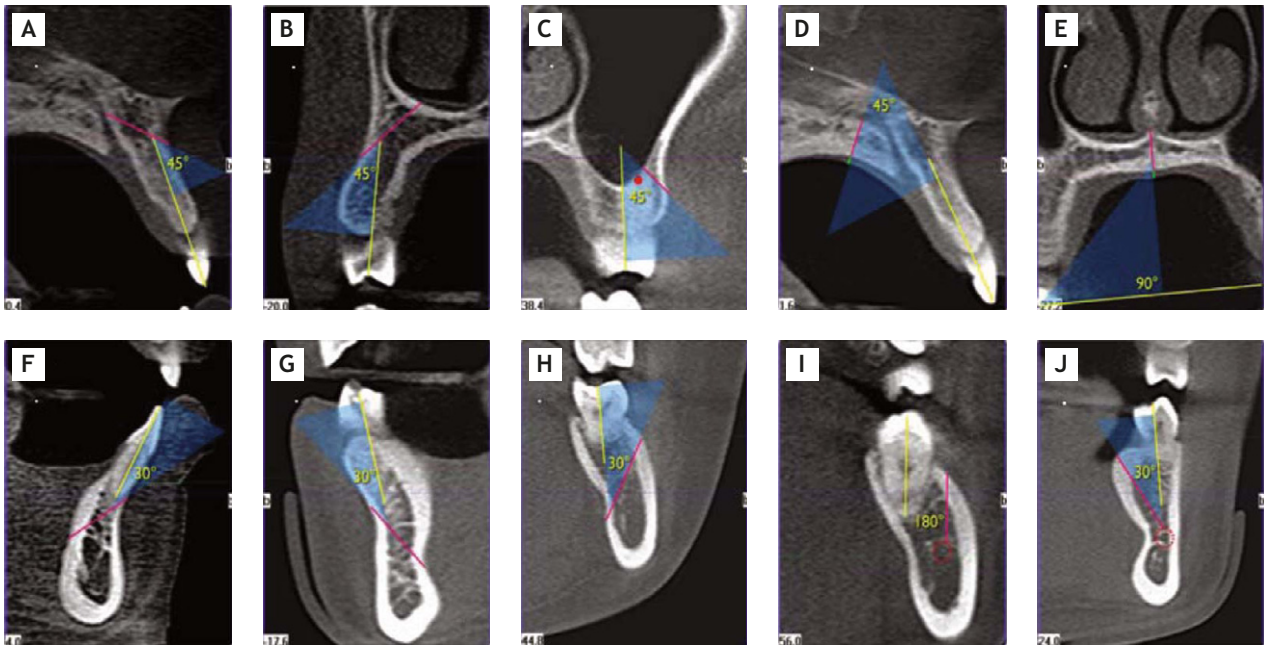

Fig. 2 Computed tomography transaxial section images of the regions of interest. (A) Incisive fossa, (B) canine fossa, (C) infrazygomatic crest, (D) premaxillary region, (E) midpalatal region, (F) symphysis, (G) canine fossa, (H) anterior external oblique ridge, (I) retromolar area, (J) sublingual fossa.

The canine fossa is limited medially by the canine eminence, inferiorly by the apex of the first premolar, and distally by the medial portion of the maxillary sinus (Figs. 2B and 3B). The IZ crest is limited distally by the zygomatic crest, inferiorly by the apex of the mesial root of the first molar, and superiorly by the medial portion of the maxillary sinus and the projecting zygomatic process (Figs. 2C and 3C). The premaxillary region is the paramedial area in the premaxilla region of the palate, limited laterally by the incisors and canine roots and medially by the incisive foramen (Figs. 2D and 3D). The midpalatal region is limited anteroposteriorly between the first and second premolars and mediolaterally by the midpalatal suture (Figs. 2E and 3E).

Mandible (4 facial and 1 lingual)

The symphysis is limited bilaterally by the canine eminences, inferiorly by the mental tubercles, and superiorly by the incisor apices (Figs. 2F and 3F). The canine fossa is limited mesially by the canine eminence, distally by the mental foramen, superiorly by the first premolar apex, and inferiorly by the mandibular inferior border (Figs. 2G and 3G).

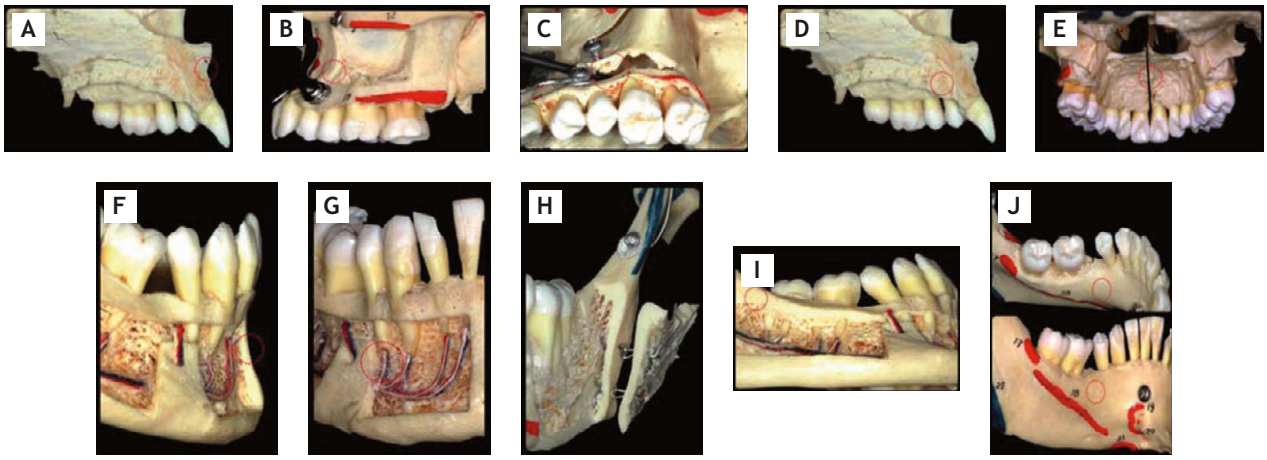

Fig. 3 Anatomic locations of regions of interest. (A) Incisive fossa, (B) canine fossa, (C) infrazygomatic crest, (D) premaxillary region, (E) midpalatal region, (F) symphysis, (G) canine fossa, (H) anterior external oblique ridge, (I) retromolar area, (J) sublingual fossa.

The AEOR is limited laterally by the external oblique ridge and medially by the crestal bone of the second molar (Figs. 2H and 3H). The retromolar area is limited mesially by the distal surface of the second molar, laterally by the external oblique ridge, and superiorly by the ascending ramus (Figs. 2I and 3I). The sublingual fossa is limited anteriorly, posteriorly, and superiorly by the apical portion of the first and second premolar roots (parallel to the tooth long axis) (Figs. 2J and 3J), and inferiorly by the mandibular inferior border.

Measurements

Reference lines for all 10 ROI measurements were established and drawn in transaxial sections at 45° on the maxilla or at 30° on the mandible relative to the long axis of the adjacent teeth, except for the retromolar area and midpalatal region.[47] In the retromolar area, the measurement was taken parallel to the long axis of the adjacent molar (Fig. 2I), while in the midpalatal region, it was taken perpendicular to the occlusal plane (Fig. 2E).

To calibrate the 10 ROI sites for each image, i-CAT Vision software was used. First, the slice control bar, found in various views and positions throughout the program, was dragged to decrease the slice thickness to 0.2 mm. Then, to make a linear measurement, the "Distance" function was selected, and a measurement in millimeters appears in the upper corner of the image. Data were the average of three measurements in the same locations by the same examiner.

Bone depths were measured for all 10 ROIs; in the meanwhile, soft-tissue depths were only quantified in the premaxillary and midpalatal regions, and the cortical bone thicknesses were measured in all other eight sites by CBCT.

Statistical analysis

Descriptive statistics included the mean, standard deviation, and minimum and maximum values, which are listed in Table 1. All statistical analyses were carried out using SPSS version 13.0 (SPSS Inc., Chicago, IL, USA). For each ROI, both the left- and right-side thicknesses (mm) were measured. Comparisons of measurements between sexes were performed with the Wilcoxon rank sum test. The Wilcoxon signed rank test was used for the paired data of labial and lingual cortical bone thicknesses, and for premaxilla and midpalatal soft-tissue thickness comparisons. All values compared with a P value <0.05 were considered to differ statistically and significantly.

Results

The data showed that there were no differences between the right and left sides ($P>0.05$) for bone depth or cortical bone thickness at each ROI. The right and left measurements were, therefore, pooled together for the descriptive statistics (Table 1).

In the comparison between sexes, there were no significant sex differences in most of the measurements, except for the cortical bone thickness of the AEOR and the lingual cortical bone thickness of the symphysis (Table 2). The cortical bone thickness of the AEOR in the male group was thicker than that of the female group ($P=0.009$); in contrast, the lingual cortical bone thickness of the symphysis in the female group was thicker than that of the male group ($P=0.046$).

Among the pairwise comparisons, the soft-tissue thickness of the premaxillary area was significantly thicker than that of the midpalatal area ($P<0.05$);

Table 1. Hard- and soft-tissue thickness measurements for each region of interest (ROI)

ROI	Bone depth (mm)				Cortical bone thickness (mm)			
	Mean	SD	Max	Min	Mean	SD	Max	Min
Maxilla								
Incisive fossa	10.41	2.69	16.2	7.4	1.92	0.33	2.5	1.3
Canine fossa	10.93	3.57	17.0	5.6	2.75	0.67	4.5	1.8
Infrazygomatic crest	5.89	3.92	18.5	3.1	1.96	0.37	3.2	1.4
Premaxillary region	10.21	2.43	14.8	7.2	4.39*	0.58	5.6	3.4
Midpalatal region	6.95	1.25	8.8	4.9	1.37*	0.31	1.7	0.8
Mandible								
Symphysis	12.79	1.6	14.5	9.1	2.11†	0.42	2.8	1.4
Symphysis (labial)					3.91†	0.69	5.0	2.7
Canine fossa	10.19	1.81	13.0	6.9	3.58	0.74	4.9	2.0
Retromolar area	14.73	2.04	17.8	10.4	4.36	1.18	7.0	2.8
Sublingual fossa	11.51	2.07	15.1	8.4	4.27	0.75	5.4	2.9

*Only the soft-tissue thicknesses were measured and compared with each other (P=0.005), not cortical bone depths; †the lingual cortical bone thickness was measured and compared with that of the labial cortex (P=0.005). SD=standard deviation; Min=minimum; Max=maximum.

and the lingual cortex thickness was thicker than that of the labial in the symphysis area ($P<0.05$) (Table 2). The perforation ratios for different TAD lengths are presented in Table 3. No perforation of the maxillary ROI was found when the length of the TAD was 6 mm, except for in the IZ crest area. In the mandibular ROI, the only possible perforation area was the canine fossa area when using an 8-mm TAD.

Discussion

Compared with traditional orthodontic radiographs, CBCT provides images without magnification and superimposition errors, and also 3D imaging and volumetric information. The versatility of CBCT to evaluate hard-tissue availability in an ROI was noted.[45,48] The soft-tissue depth evaluation is recorded by piercing the mucosa with a needle until the attached rubber stop rests on the mucosa.[49,50] By adjusting the tissue threshold, the soft-tissue thickness can be easily measured from the CBCT image with no invasive clinical procedures. The 3D image is reconstructed by discrete data divided into voxels; although inadvertent selection of the nearest neighbor point occurs, a minimal voxel size helps reduce such errors.[51] In addition, the amount of CBCT radiation the patient receives is less than that with other types of tomography.[52]

TAD insertion sites can be divided into two categories: inter-radicular and extra-alveolar areas. Extra-alveolar insertion sites, which can minimize the risks of root injury,[2,34,53] might allow the force direction to be closer to the center of resistance in some situations.[4,18]

Another substantial issue in this study is the TAD insertion angle, which can directly influence the available depth of the hard tissue. Clinically, in order not to cause root injuries, it is easier for clinicians to use the long axis of neighboring teeth as a guide to perform insertion of a TAD. Therefore, all insertion angles for each ROI mentioned in this study were based on previous studies with the neighboring teeth as a guide.[9,13,46]

In the present study, the average bone depths were around or >10 mm, except for the IZ crest and midpalatal region; the average cortical bone thicknesses were around or >2 mm, except for the incisive fossa, IZ crest, and midpalatal region (Table 1). The bone depth of the IZ crest should be at least 6 mm to adequately sustain a miniscrew throughout treatment.[46] The average bone depth of the IZ crest in this study was 5.89 mm; the bone depth of the IZ crest in the male group was longer than 6 mm, but not that in the female group (Table 2). It was supposed that the variation in IZ crest thickness might be due to variations in the maxillary sinus among individuals.[54] There was no sex difference ($P=0.09$) in the cortical bone thickness of the IZ crest.

In a previous study based on 20 Caucasian males, the recommended lengths of the TAD for the maxillary incisive fossa and symphysis differed.[13] The length of the TAD for the symphysis could be longer than that of the incisive fossa in white males. Similar results were also found in our study. The mean bone depth was thicker at the symphysis than the incisive fossa (Table 1).

Table 2. Hard- and soft-tissue thickness measurements in each region of interest (ROI) between sexes

ROI	Bone thickness (mm)									Cortical bone thickness (mm)								
	Male				Female				P	Male				Female				P
	Mean	Max	Min	SD	Mean	Max	Min	SD		Mean	Max	Min	SD	Mean	Max	Min	SD	
Maxilla																		
Incisive fossa	11.30	16.2	7.4	3.68	9.52	11.0	8.5	0.91	0.60	1.74	2.0	1.3	0.30	2.10	2.5	1.8	0.26	0.08
Canine fossa	10.69	17.0	5.6	4.00	11.16	15.6	6.1	3.28	0.92	2.79	4.5	1.8	0.80	2.71	3.8	2.0	0.56	0.67
IZ ridge	7.25	18.5	3.4	5.22	4.52	6.2	3.1	0.99	0.34	2.05	3.2	1.7	0.44	1.86	2.3	1.4	0.29	0.09
Premaxillary region*	9.50	11.8	7.5	1.97	10.92	14.8	7.2	2.86	0.47	4.68	5.6	4.1	0.58	4.10	4.7	3.4	0.47	0.11
Midpalatal region*	6.66	8.8	4.9	1.56	7.24	8.4	6.1	0.93	0.46	1.24	1.6	0.8	0.30	1.50	1.7	1.0	0.28	0.13
Mandible																		
Symphysis	12.98	14.5	11.2	1.30	12.60	14.1	9.1	1.99	0.92	1.96	2.3	1.4	0.38	2.26	2.8	1.7	0.44	0.40
Symphysis (L)†										3.50	4.3	2.7	0.60	4.32	5.0	3.7	0.54	0.046
Canine fossa	10.98	13.0	8.7	1.44	9.40	12.8	6.9	1.85	0.17	3.87	4.9	2.8	0.74	3.29	4.0	2.0	0.65	0.53
AEOR	14.00	16.4	12.0	1.68	12.48	13.9	9.5	1.19	0.14	4.33	5.1	3.3	0.58	3.59	4.8	2.7	0.55	0.009
Retromolar area	15.67	17.6	13.2	1.37	13.78	17.8	10.4	2.21	0.11	4.78	7.0	3.6	1.40	3.94	4.8	2.8	0.78	0.45
Sublingual fossa	10.84	13.3	8.4	1.81	12.18	15.1	9.3	2.19	0.60	4.37	5.4	2.9	0.75	4.16	5.1	3.1	0.77	0.29

*Only the soft tissue thicknesses were measured, not the cortical bone depths; †lingual cortical bone thickness was measured. SD=standard deviation; Max=maximum; Min=minimum; IZ=infrazygomatic; AEOR=anterior external oblique ridge.

Table 3. Numbers and ratio of perforations for incremental length of the temporary anchorage devices

ROI	4 mm		6 mm		8 mm		10 mm		12 mm	
	No.	%	No.	%	No.	%	No.	%	No.	%
Maxilla										
Incisive fossa*	0/10	0	0/10	0	1/10	10	6/10	60	8/10	80
Canine fossa†	0/20	0	1/20	5	5/20	25	9/20	45	11/20	55
Infrazygomatic crest†	6/20	30	16/20	80	18/20	90	18/20	90	18/20	90
Premaxillary region*	0/10	0	0/10	0	3/10	30	5/10	50	8/10	80
Midpalatal region*	0/10	0	2/10	20	8/10	80	10/10	100	10/10	100
Mandible										
Symphysis*	0/10	0	0/10	0	0/10	0	1/10	10	2/10	20
Canine fossa†	0/20	0	0/20	0	2/20	10	9/20	45	17/20	85
AEOR†	0/20	0	0/20	0	0/20	0	1/20	5	3/20	15
Retromolar area†	0/20	0	0/20	0	0/20	0	0/20	0	3/20	15
Sublingual fossa†	0/20	0	0/20	0	0/20	0	5/20	25	13/20	65

*Single sites; †dual sites, including both right and left sides. AEOR = anterior external oblique ridge.

The cortical bone thickness of the lingual symphysis and AEOR showed a significant difference between sexes. The female lingual symphysis cortex was thicker than that of males, whereas males had a thicker cortex in the AEOR (Table 2). A recent study also reported that the cortex was thinner in females than in males in the posterior buccal regions.[55]

To adequately sustain a TAD throughout treatment, a mechanical lock is needed, rather than bone integration as with dental implants. The amount of cortical bone in contact with the TAD threads plays an important role in mechanical locking.[56] Furthermore, this mechanical lock can be either a unicortical or bicortical anchorage. A unicortical anchorage means that the TAD penetrates only one cortical plate, whereas with bicortical anchorage, the TAD is long enough to penetrate two cortical plates. For example, if the TAD is long enough, it can penetrate the buccal cortical plate and bone marrow and embed into the lingual cortical plate at the symphysis. Clinically, it is important for clinicians to be familiar with the anatomy of TAD insertion sites. When a unicortical anchorage is needed, a TAD length of up to 10 mm is not recommended for all ROIs, except in the retromolar area. As for bicortical anchorage, the clinician must know the exact bone depth to prevent soft-tissue perforation on the opposite side.

As to soft-tissue concerns, TADs are inserted in the keratinized gingival tissue area and designed with a smooth neck for most applications.[9] However, placing a TAD in some extra-alveolar areas could potentially cause mucosal inflammation. Although a specially designed appliance was used to prevent associated problems, a complicated design can cause food impaction and discomfort.[13] Another way to prevent inflammation is to place the TAD in the mobile mucosa, that is, cover the screw head beneath the mucosa with an extension for force application. In the presented results, the premaxillary soft tissue was statistically thicker than that of the midpalate, showing that a TAD with a longer smooth neck design should be considered in the premaxillary region.

In conclusion, CBCT provides a better clinical evaluation than traditional radiographs. The results validate these 10 extra-alveolar regions as being safe host sites for a TAD. In order to reduce the risks of perforation, different lengths of TADs ranging 6–10 mm are recommended for these 10 ROIs. The soft tissue depth in the palatal area is thicker in the premaxillary than the midpalatal region. The design of TADs for different ROIs should take both hard- and soft-tissue thicknesses into considerations to reduce clinical complications. As for the length selection of TADs, individual evaluation should be of concern to clinicians.

References

1. Roberts WE, Nelsen CL, Goodacre CJ. Rigid implant anchorage to close a mandibular first molar extraction site. *J Clin Orthod* 1994;38:693–704.
2. Umemori M, Sugawara J, Mitani H, Nagasaka H, Kawamura H. Skeletal anchorage system for open-bite correction. *Am J Orthod Dentofacial Orthop* 1999;115:166–74.
3. Kuroda S, Katayama A, Takano-Yamamoto T. Severe anterior open-bite case treated using titanium screw anchorage. *Angle Orthod* 2004;74:558–67.
4. Costa A, Raffainl M, Melsen B. Miniscrews as orthodontic anchorage: a preliminary report. *Int J Adult Orthodon Orthognath Surg* 1998;13:201–9.
5. Kanomi R. Mini-implant for orthodontic anchorage. *J Clin Orthod* 1997;31:763–7.

6. Park YC, Lee SY, Kim DH, Jee SH. Intrusion of posterior teeth using mini-screw implants. *Am J Orthod Dentofacial Orthop* 2003;123:690–4.
7. Park HS, Kwon DG, Sung JH. Nonextraction treatment with microscrew implant. *Angle Orthod* 2004;74:539–49.
8. Melsen B, Costa A. Immediate loading of implants used for orthodontic anchorage. *Clin Orthod Res* 2000;3:23–8.
9. Melsen B. Mini-implants: where are we? *J Clin Orthod* 2005; 39:539–47.
10. Deguchi T, Nasu M, Murakami K, Yabuuchi T, Kamioka H, Takano-Yamamoto T. Quantitative evaluation of cortical bone thickness with computed tomographic scanning for orthodontic implants. *Am J Orthod Dentofacial Orthop* 2006; 129:721.e7–12.
11. Poggio PM, Incorvati C, Velo S, Carano A. "Safe zones": a guide for miniscrew positioning in the maxillary and mandibular arch. *Angle Orthod* 2006;76:191–7.
12. Kim HJ, Yun HS, Park HD, Kim DH, Park YC. Soft-tissue and cortical-bone thickness at orthodontic implant sites. *Am J Orthod Dentofacial Orthop* 2006;130:177–82.
13. Costa A, Pasta G, Bergamaschi G. Intraoral hard and soft tissue depths for temporary anchorage devices. *Semin Orthod* 2005;11:10–5.
14. Cousley RR, Parberry D. Surgical stents for accurate miniscrew insertion. *J Clin Orthod* 2006;40:412–7.
15. Barros SE, Janson G, Chiqueto K, Freitas M, Henriques J, Pinzan A. A three-dimensional radiographic-surgical guide for mini-implant placement. *J Clin Orthod* 2006;40: 548–54.
16. Bae SM, Park HS, Kyung HM, Kwon OW, Sung JH. Clinical application of micro-implant anchorage. *J Clin Orthod* 2002; 36:298–302.
17. Kyung SH, Choi JH, Park YC. Miniscrew anchorage used to protract lower second molars into first molar extraction sites. *J Clin Orthod* 2003;37:575–9.
18. Carano A, Velo S, Leone P, Siciliani G. Clinical applications of the Miniscrew Anchorage System. *J Clin Orthod* 2005;39:9–24.
19. Maino BG, Bednar J, Pagin P, Mura P. The spider screw for skeletal anchorage. *J Clin Orthod* 2003;37:90–7.
20. Kyung HM, Park HS, Bae SM, Sung JH, Kim IB. Development of orthodontic micro-implants for intraoral anchorage. *J Clin Orthod* 2003;37:321–8.
21. Kitai N, Yasuda Y, Takada K. A stent fabricated on a selectively colored stereolithographic model for placement of orthodontic mini-implants. *Int J Adult Orthodon Orthognath Surg* 2002;17:264–6.
22. Freudenthaler JW, Haas R, Bantleon HP. Bicortical titanium screws for critical orthodontic anchorage in the mandible: a preliminary report on clinical applications. *Clin Oral Implants Res* 2001;12:358–63.
23. Sato S, Arai Y, Shinoda K, Ito K. Clinical application of a new cone-beam computerized tomography system to assess multiple two-dimensional images for the preoperative treatment planning of maxillary implants: case reports. *Quintessence Int* 2004;35:525–8.
24. Clark DE, Danforth RA, Barnes RW, Burtch ML. Radiation absorbed from dental implant radiography: a comparison of linear tomography, CT scan, and panoramic and intraoral techniques. *J Oral Implantol* 1990;16:156–64.
25. Ekestubbe A, Thilander A, Grondahl K, Grondahl HG. Absorbed doses from computed tomography for dental implant surgery: comparison with conventional tomography. *Dentomaxillofac Radiol* 1993;22:13–7.
26. Lecomber AR, Yoneyama Y, Lovelock DJ, Hosoi T, Adams AM. Comparison of patient dose from imaging protocols for dental implant planning using conventional radiography and computed tomography. *Dentomaxillofac Radiol* 2001;30: 255–9.
27. Ngan DC, Kharbanda OP, Geenty JP, Darendeliler MA. Comparison of radiation levels from computed tomography and conventional dental radiographs. *Aust Orthod J* 2003; 19:67–75.
28. Crismani AG, Bernhart T, Bantleon HP, Cope JB. Palatal implants: the Straumann Orthosystem. *Semin Orthod* 2005; 11:16–23.
29. Mah J, Hatcher DC. Current status and future needs in craniofacial imaging. *Orthod Craniofac Res* 2003;6(Suppl 1): 10–6.
30. Mah JK, Danforth RA, Bumann A, Hatcher D. Radiation absorbed in maxillofacial imaging with a new dental computed tomography device. *Oral Surg Oral Med Oral Pathol Oral Radiol Endod* 2003;96:508–13.
31. Ludlow JB, Davies-Ludlow LE, Brooks SL. Dosimetry of two extraoral direct digital imaging devices: NewTom cone beam CT and Orthophos Plus DS panoramic unit. *Dentomaxillofac Radiol* 2003;32:229–34.
32. Hung J, Bumann A, Mah J. Three-dimensional radiographic analysis in orthodontics. *J Clin Orthod* 2005;39:421–8.
33. Borah GL, Ashmead D. The fate of teeth transfixed by osteosynthesis screw. *Plast Reconstr Surg* 1996;97:726–9.
34. Lee KJ, Joo E, Kim KD, Lee JS, Park YJ, Yu HS. Computed tomographic analysis of tooth-bearing alveolar bone for orthodontic miniscrew placement. *Am J Orthod Dentofacial Orthop* 2009;135:486–94.
35. Costa A, Levrini L, Tagliabue A. Osteointegrazione negli impianti come ancoraggio ortodontico. *Ital J Oral Implantol* 2000;2:133–9.
36. Xun C, Zeng X, Wang X. Microscrew anchorage in skeletal anterior open-bite treatment. *Angle Orthod* 2007;77: 47–56.
37. Melsen B, Verna C. Miniscrew implants: the Aarhus anchorage system. *Semin Orthod* 2005;11:24–31.
38. Giancotti A, Arcuri C, Barlattani A. Treatment of ectopic mandibular second molar with titanium miniscrews. *Am J Orthod Dentofacial Orthop* 2004;126:113–7.
39. Kinzinger GS, Diedrich PR, Bowman SJ. Upper molar distalization with a miniscrew-supported distal jet. *J Clin Orthod* 2006;40:672–8.
40. Sugawara J, Daimaruya T, Umemori M, et al. Distal movement of mandibular molars in adult patients with the skeletal anchorage system. *Am J Orthod Dentofacial Orthop* 2004; 125:130–8.
41. Dalstra M, Cattaneo PM, Melsen B. Load transfer of miniscrews for orthodontic anchorage. *Orthodontics* 2004;1: 53–62.
42. Frost HM. Perspectives: bone's mechanical usage windows. *Bone Miner* 1992;19:257–71.
43. Jonasson G, Kiliaridis S, Gunnarsson R. Cervical thickness of the mandibular alveolar process and skeletal bone mineral density. *Acta Odontol Scand* 1999;57:155–61.
44. Sarikaya S, Haydar B, Ciğer S, Ariyürek M. Changes in alveolar bone thickness due to retraction of anterior teeth. *Am J Orthod Dentofacial Orthop* 2002;122:15–26.
45. King KS, Lam EW, Faulkner MG, Heo G, Majore PW. Vertical bone volume in the paramedian palate of adolescents: a computed tomography study. *Am J Orthod Dentofacial Orthop* 2007;132:783–8.
46. Liou EJ, Chen PH, Wang YC, Lin JC. A computed tomographic image study on the thickness of the infrazygomatic crest of the maxilla and its clinical implications for miniscrew insertion. *Am J Orthod Dentofacial Orthop* 2007;131:352–6.
47. Moore KL. The head. In: Moore KL, ed. *Clinically Oriented Anatomy*, 2nd ed. Baltimore: Williams & Wilkins, 1985: 794–982.
48. Siwerdsen JH, Jaffray DA. Cone-beam computed tomography with a flat-panel imagery. *Med Phys* 1999;26:2635–47.

49. Wara-aswapati N, Pitiphat W, Chandrapho N, Rattanayatikul C, Karimbux N. Thickness of palatal masticatory mucosa associated with age. *J Periodontol* 2001;72:1409–12.
50. Schulze R, Curiè D, d'Hoedt B. B-mode versus A-mode ultrasonographic measurements of mucosal thickness in vivo. *Oral Surg Oral Med Oral Pathol* 2002;93:1.
51. Patera J. *Iso-surface Extraction and Approximation Error* (Technical Report DCSE/TR-2004-15). Plzen, Czek Republic: Centre of Computer Graphics and Data Visualisation, Department of Computer Science and Engineering, University of West Bohemia, 2004.
52. Mozzo P, Procacci C, Tacconi A, Martini PT, Andreis IA. A new volumetric CT machine for dental imaging based on the cone beam technique: preliminary results. *Eur Radiol* 1998;8:1558–64.
53. Ohmae M, Saito S, Morohashi T, et al. A clinical and histological evaluation of titanium mini-implants as anchors for orthodontic intrusion in the beagle dog. *Am J Orthod Dentofacial Orthop* 2001;119:489–97.
54. Eberhardt JA, Torabinejad M, Christiansen EL. A computed tomographic study of the distances between the maxillary sinus floor and the apices of the maxillary posterior teeth. *Oral Surg Oral Med Oral Pathol Oral Radiol Endod* 1992;73:345–7.
55. Ono A, Motoyoshi M, Shimizu N. Cortical bone thickness in the buccal posterior region for orthodontic mini-implants. *Int J Oral Maxillofac Surg* 2008;37:334–40.
56. Monnerat C, Restle L, Mucha JN. Tomographic mapping of mandibular interradicular spaces for placement of orthodontic mini-implants. *Am J Orthod Dentofacial Orthop* 2009; 135:428–9.

J Dent Sci 2010;5(1):30–35

ORIGINAL ARTICLE

Enhancement of 5-aminolevulinic acid-induced photodynamic therapy by a bioadhesive polymer

*Shu-Fang Chang,[1] Yu-Tsai Yang,[2] Wei-Ling Li,[3] Che-Tong Lin,[2] Tsuimin Tsai[2,3]**

[1]Department of Dentistry, Shin Kong Wu Ho-Su Memorial Hospital, Taipei, Taiwan
[2]College of Oral Medicine, Taipei Medical University, Taipei, Taiwan
[3]Graduate Institute of Biomedical Materials and Engineering, Taipei Medical University, Taipei, Taiwan

Received: Nov 14, 2009
Accepted: Feb 20, 2010

KEY WORDS:
aminolevulinic acid;
Carbopol;
photodynamic therapy;
protoporphyrin IX

Background/purpose: Using a topical formulation of 5-aminolevulinic acid (ALA), a mediated photodynamic therapy (PDT) was developed to treat oral precancerous and cancerous lesions. Several clinical results demonstrated that this special ALA preparation containing Carbopol 971P (CP971P), a bioadhesive polymer, resulted in a satisfactory PDT effect. It is believed that this PDT efficacy may be due to the increased bioadhesion of the preparation at the treatment site. We investigated whether there was a beneficial effect of CP971P on ALA PDT *in vitro*.
Materials and methods: CP971P was co-incubated with ALA in a cell culture system. The effect of CP971P was evaluated by monitoring the uptake of ALA, the fluorescence intensity of protoporphyrin IX, and the cell survival rate.
Results: The polymer was found to enhance the fluorescence intensity of protoporphyrin IX and the subsequent PDT effect when concurrently dosed with ALA.
Conclusion: Our results showed that a formulation of ALA containing C971P could provide a better ALA PDT effect in cancer treatment.

Introduction

Photodynamic therapy (PDT) is a new treatment modality in which a combination of a photosensitizer and visible light is programmed to result in the destruction of selected cells. In 1987, Malik and Lugaci[1] first reported the used of endogenous protoporphyrins as clinical photosensitizing agents. Later in 1990, Divaris et al.[2] proposed a new approach to PDT, which involves the photosensitizer prodrug, 5-aminolevulinic acid (ALA). ALA is a metabolic prodrug of protoporphyrin IX (PpIX), a photosensitizing agent, in the heme biosynthesis pathway. Endogenous synthesis of ALA is regulated by the synthesis of heme via feedback control; following the exogenous administration of ALA, the feedback mechanism is bypassed with subsequent overproduction and accumulation of porphyrin precursors, the predominant one of which is PpIX.[3] The use of PpIX generated through the heme biosynthetic pathway after administration of ALA has many applications in PDT against various cancers.[4,5] A simplified

*Corresponding author. Graduate Institute of Biomedical Materials and Engineering, Taipei Medical University, 250, Wu-Hsing Street, Taipei 11042, Taiwan.
E-mail: tmtsai00@tmu.edu.tw

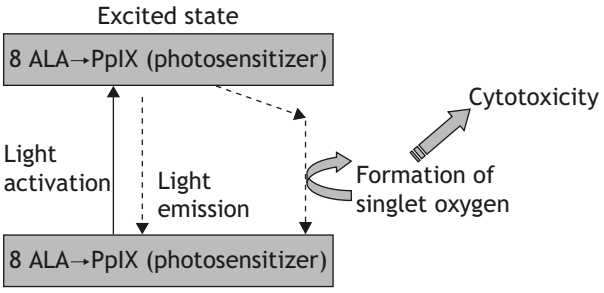

Fig. 1 Schematic expression of the mechanism of 5-aminolevulinic acid (ALA) photodynamic therapy (PDT). Eight ALA molecules form one protoporphyrin IX (PpIX) molecule via the heme biosynthesis pathway. Upon suitable light exposure, the ground state of PpIX can jump to a higher energy state (excited state). When an oxygen molecule is available, formation of singlet oxygen through energy transfer from the excited PpIX can be used to induce cellular damage.

schematic expression of ALA PDT is shown in Fig. 1. The formation of one PpIX molecule requires eight ALA molecules for synthesis. Selective PpIX accumulation may be related to several factors, such as increased uptake of ALA, a low concentration of iron, a low activity of ferrochelatase, and a high activity of porphobilinogen deaminase in tumor cells.[6] The passage of ALA through the cell membrane is restricted by the rate of uptake by neoplastic cells and its poor diffusion through tissues and cellular membranes.[3] In order to increase its transport across cellular membranes, rather high concentrations of ALA generally must to be applied over long periods of time. Except for the Levulan Kerastick Topical Solution[7] and a sol-gel preparation,[8–10] the reasons for including any single vehicle material in the formulation of most ALA formulations published in the literature were not explained. The Levulan Kerastick Topical Solution and the sol-gel preparation showed comparatively better ALA PDT results in clinical treatments, and the reason may have been due to a rational formulation design that ensured the performance of ALA and the formation the photosensitizer, PpIX, and a subsequent PDT effect upon irradiation. The Levulan Kerastick Topical Solution is a two-component system: one component containing 1.5 mL of solution vehicle, and the other component containing 354 mg of ALA HCl as a dry solid. The reason for the two-component system is mainly due to stability concerns with ALA. ALA is not stable in solution and easily undergoes dimerization, so it is better to keep it in a dry powder form during storage. Since the Levulan Kerastick Topical Solution is mainly for skin application, the solution vehicle they include in the preparation is basically for enhancing penetration of ALA through the skin. The target of the sol-gel preparation is the oral mucosa, and a combination of a mucoadhesive polymer and thermal-responsive polymer is included to enhance the retention time of ALA at the application site in order to increase drug uptake at the target site.[8–10] Recently, the ALA sol-gel formulation was reported to exert a satisfactory result for skin wart treatment.[11] In that report, the authors reportedly achieved a complete response 3 weeks after ALA PDT, and no recurrence was observed for up to 2 years in 94% of patients. However, the reason d this clinical result using the ALA sol-gel was better than those using ALA cream[12] is not clear.

Recently, a new field of "polymer therapeutics" has garnered lots of attention for pharmaceutical formulators, and mucoadhesive polymers seem to have the potential to enhance the performance of active ingredients.[13] It would be interesting to study whether the mucoadhesive polymer, Carbopol 971P (CP971P), in the ALA sol-gel preparation[8–11] holds the answer as to why the sol-gel formulation showed a better PDT effect than the traditionally favored cream preparation.[12] Carbopol polymers (including CP971P) are generally regarded as safe polymers composed of acrylic acid crosslinked with polyalkenyl ethers or divinyl glycol.[14] Carbopol polymers are commonly used in oral suspensions, tablets, and topical formulations, and their mucoadhesive properties provide intimate contact between the dosing formulation and the mucosal surface, resulting in prolonged residence time at the site of absorption. Since the clinical results demonstrated that the ALA sol-gel preparation can produce a satisfactory PDT effect on oral cancers and precancerous lesions,[8–10] it would be interesting to know whether such a formulation can benefit other mucous routes, such as the lung. In this study, the effect of CP971P on a PpIX formation and the subsequent PDT effect after incubation with ALA in cell culture systems were studied.

Materials and methods

Cell culture conditions and ALA incubation

Two cell lines were tested for the effect of CP971P on ALA PDT. KB cells (ATCC CCL-17; American Type Culture Collection, Manassas, VA, USA), originally obtained from an epidermal carcinoma of the mouth, were cultured in Eagle's minimum essential medium (Sigma, St. Louis, MO, USA) with 10% fetal bovine serum (FBS) (Gibco, Gaithersburg, MD, USA). CL1-0 cells, established from a 64-year-old man with a poorly differentiated lung adenocarcinoma, were kindly provided by the National Health Research Institutes (Miaoli, Taiwan). A stock culture of CL1-0 cells was maintained in RPMI 1640 (Sigma) with 10% FBS. Cell cultures were maintained at 37ºC in a

humidified atmosphere of 95% air and 5% CO_2. The cells seeded in culture plates or dishes were incubated with 1mM ALA (with or without CP971P, diluted in serum-free medium and neutralized to pH 7.2 with NaOH immediately before use) for 3 hours. CP971P was kindly provided by Lubrizol (Wickliffe, OH, USA), and a stock solution (1% wt/vol) was prepared by slowly adding the polymer powder into water with stirring for 3 hours or longer. Various concentrations of CP971P were obtained by taking aliquots of the stock solution and diluting them with water.

Measurement of ALA-induced PpIX fluorescence by flow cytometry

Cells were seeded in triplicate in six-well plates containing 2×10^5 cells per well and incubated for 24 hours at 37°C. Afterwards, cells were incubated in phenol red-free, serum-free medium containing 1mM ALA for 3 hours. Following ALA incubation, cells were trypsinized, removed from the culture dishes, and resuspended in fresh culture medium supplemented with serum. Cellular fluorescence was quantified with a Coulter EPICS XL-MCL flow cytometer (Beckman Coulter, Miami, FL, USA), and 10,000 cells were analyzed. The ALA-induced photosensitizer, PpIX, was excited by an argon ion laser emission at 488 nm and collected by a photomultiplier tube after passing through a 670-nm long-pass filter.

Photodynamic treatment

For photodynamic treatment, cells were seeded in 96-well plates (at about 6000 cells/well) and grown overnight in complete medium. After incubation with 1mM ALA with or without 0.05% CP971P for 3 hours, cells were exposed to light at doses of 0–32 J/cm^2. The light source was a light-emitting diode at 60 mW, with a wavelength emission of red light at 630±5 nm. After irradiation, cells were incubated with fresh complete medium for another 24 hours until further analysis.

Cell viability assay

The PDT-induced phototoxicity of test cells was determined by the 3-(4,5-dimethylthiazol-2-yl)-2,5-diphenyltetrazolium bromide (MTT) assay. Each individual phototoxic experiment was performed in triplicate. The MTT assay is based on the activity of mitochondrion dehydrogenase, which can reduce a water-soluble tetrazolium salt to a purple insoluble formazan product.[15] The resulting formazan crystals were dissolved by the addition of dimethyl sulfoxide, and analyzed spectrophotometrically at an absorbance of 570 nm. Cells exposed to ALA but without light were used as the control. The cell survival rate (%) was calculated as: (mean optical density value of treated cells/mean optical density value of control cells)×100%.

Determination of ALA uptake

[^{14}C]ALA hydrochloride was purchased from New England Nuclear (Boston, MA, USA) and used in this part of the study. Unlabelled ALA was dissolved in phosphate-buffered saline (PBS), and [^{14}C]ALA was added so that the final solution contained 0.0222 MBq/mL. Cells were washed twice with 0.5 mL PBS at 37°C and incubated with 0.3 mL radiolabeled ALA solution in the culture medium without FBS. At certain time intervals, the reaction was stopped, and cells were washed four times with 0.5 mL ice-cold PBS. Cells were then disrupted in 0.2mM NaOH and transferred to vials containing 5 mL cocktail scintillation fluid (Beckman Ready Protein; Beckman Instruments, Fullerton, CA, USA). The radioactive content of the samples was determined by a Beckman LS 1801 counter (Beckman Instruments, Karlsruhe, Germany)[16]. Data are expressed as the apparent ALA concentration in pmol/mg of protein, calculated from the amount of radioactivity in cells.

Statistical analysis

Data are presented as the mean±standard error of the mean. At least three independent experiments were performed for each experiment. An unpaired *t* test was used to establish the significance of differences between groups. Differences were considered statistically significant at $P<0.05$.

Results and Discussion

The effect of CP971P on the relative fluorescence of ALA-converted PpIX in CL1-0 cells is shown in Fig. 2. The fluorescence intensity was measured by flow cytometry after incubation with 1mM ALA in the presence or absence of CP971P for 3 hours. As shown in Fig. 2, in the presence of CP971P, the fluorescence intensity increased in a concentration-dependent manner until it reached a plateau at 0.05%. A further increase in the CP971P concentration to 0.1% did not further increase the fluorescence intensity. In fact, the PpIX fluorescence intensity of cells treated with 0.05% CP971P was almost double that without CP971P. A similar effect of CP971P on the formation of PpIX was found with oral epithelial carcinoma cells, and the results are given in Table 1. For KB cells, even 0.001% CP971P showed 23% enhancement of the PpIX fluorescence. The higher fluorescence intensity indicated that

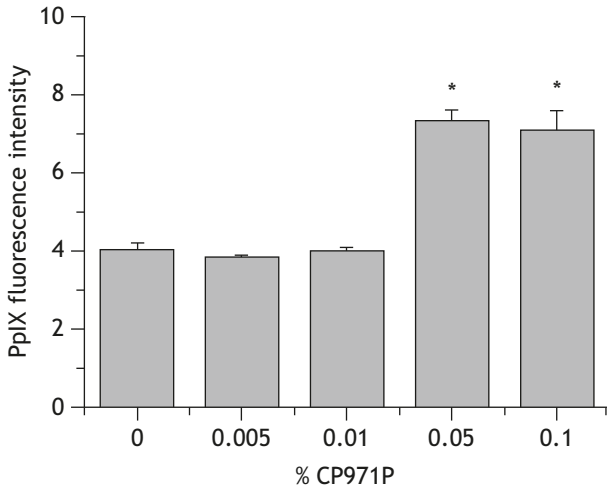

Fig. 2 Effect of Carbopol 971P (CP971P) on 5-aminolevulinic acid (ALA)-induced relative fluorescence of protoporphyrin IX (PpIX) in CL1-0 cells measured by flow cytometry. Cells were measured after incubation with 1mM ALA with various concentrations of CP971P for 3 hours. The PpIX fluorescence was acquired by flow cytometry. *$P<0.01$.

Table 1. Effect of Carbopol 971P (CP971P) on the fluorescence intensity of protoporphyrin IX (PpIX) in KB cells incubated with 1mM 5-aminolevulinic acid (ALA) for 3 hours

Cells incubated with 1mM ALA for 3 hours	Increased PpIX fluorescence intensity (%)	P
No CP971P	0	
0.001% CP971P	23	<0.05
0.01% CP971P	33	<0.05

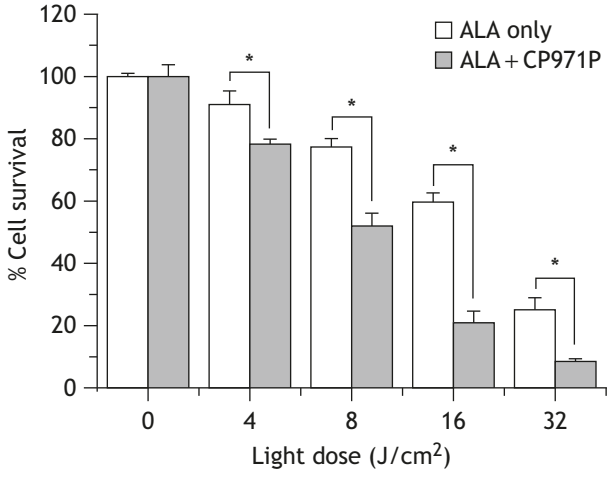

Fig. 3 Presence of 0.05% Carbopol 971P (CP971P) and light dose dependency of 5-aminolevulinic acid (ALA) photodynamic therapy on the survival rate of CL1-0 cells using the MTT assay. Cells were incubated with 1mM ALA for 3 hours and subjected to various doses of light illumination. *$P<0.01$.

more ALA-converted PpIX was present in the presence of CP971P, suggesting that more reactive oxygen species were produced to kill cancer cells after light irradiation. However, it should be noted that KB cells were shown to be contaminated by HeLa cells.[17] In this regard, it is necessary to perform more studies in other representative cell lines derived from oral squamous cell carcinoma.

To examine the efficacy of PDT, an MTT assay was performed to evaluate the cell-killing effect. As shown above, 1 mM ALA combined with 0.05% CP971P showed the strongest PpIX fluorescence. Therefore, the possible increased efficacy of PDT by CP971P was evaluated using this condition, and the results are shown in Fig. 3. In the absence of CP971P, the cell survival rate decreased in a light-dose relationship as expected. In the presence of 0.05% CP971P, the cell survival rate still showed a decreasing tendency with an increasing light dose. However, inclusion of 0.05% CP971P in the ALA PDT study resulted in a more significant enhancement of cell death, especially at the light dose ranges of 8 and 16 J/cm^2. Cell survival rates without CP971P were around 80% and 60% under light doses of 8 and 16 J/cm^2, respectively. However, in the presence of CP971P, the cell survival rate was down to 50% and 20% under light doses of 8 and 16 J/cm^2, respectively. The result is not surprising, because the presence of CP971P was found to increase the formation of PpIX. An increase in the photosensitizer is expected to increase the phototoxicity of cells where the photosensitizer resides. The results of the increased PpIX fluorescence and enhanced killing effect by adding a trace amount of a common polymer (such as Carbopol) are encouraging and of high potential in drug development. If PDT's efficacy can be improved simply by adding a much cheaper polymer concurrently with the photosensitizer, the formulator can utilize such information and design a less expensive drug for PDT.

The conversion of ALA to PpIX was correlated with several steps, including the amount of ALA transported into cells and the activity of several enzymes involved in the heme synthesis pathway (Fig. 4). CP971P is a macromolecular polymer with an average molecular weight of 10^6 kDa, and its penetration through cell membranes is almost impossible. Therefore, the enhancement of PpIX fluorescence, as well as ALA-PDT's effect, could have been due to an increase in the passive diffusion of ALA into cells or the active uptake of ALA by cells in the presence of CP971P. By tracing the intensity of labeled ALA in cells after 3 hours of incubation and removal of the culture medium, it was found that the uptake of ALA by CL1-0 cells was greatly enhanced in the presence of CP971P in the system as shown in Fig. 5. In the presence of CP971P, ALA

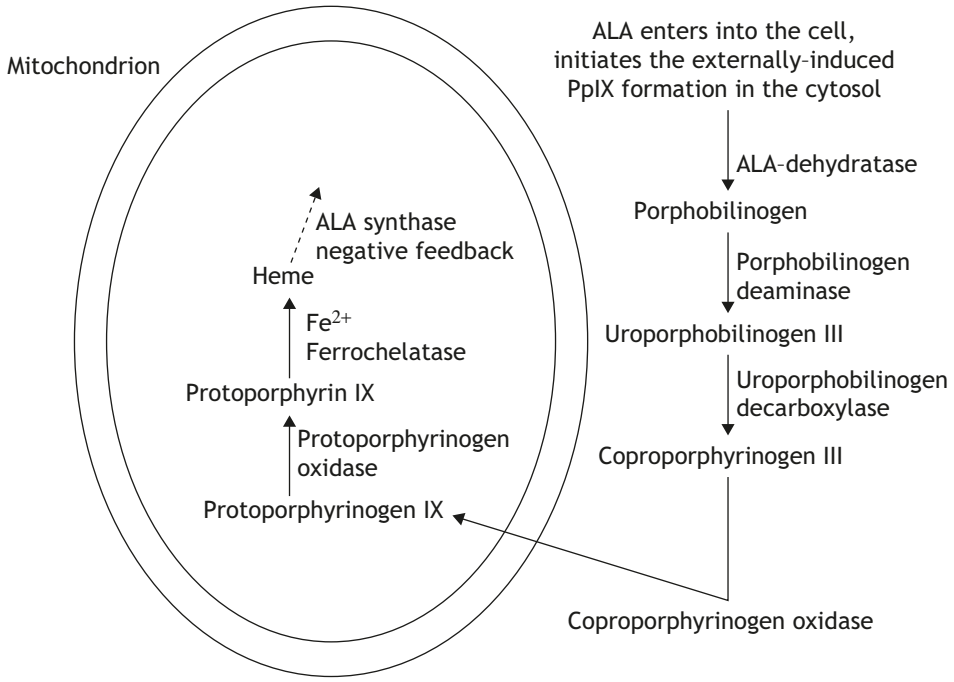

Fig. 4 Schematic expression of the formation of protoporphyrin IX (PpIX) through the heme formation pathway after external dosing of 5-aminolevulinic acid (ALA). The biosynthesis of heme occurs partly in the mitochondria and partly in the cytosol. PpIX is originally synthesized in the mitochondria.

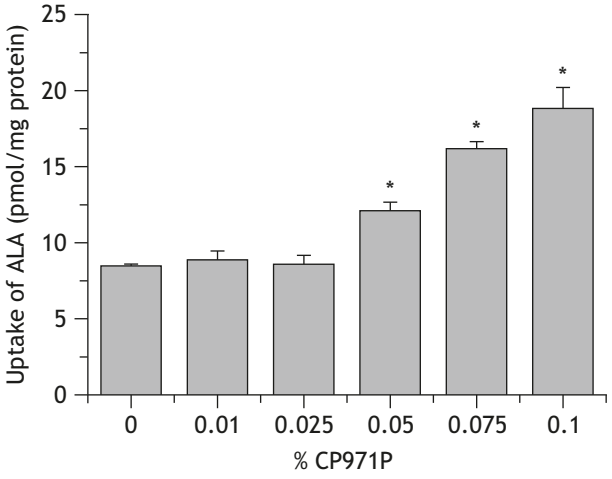

Fig. 5 Presence of Carbopol 971P (CP971P) on the uptake of 5-aminolevulinic acid (ALA) by CL1-0 cells with 3 hours of incubation time. Cells were incubated with 1mM ALA (a mixture of cold and hot ALA, labeled with ^{14}C) with various concentrations of CP971P for 3 hours. *$P<0.01$.

uptake increased in a concentration-dependent manner. This result is consistent with the increased PpIX fluorescence intensity, where the PpIX fluorescence also showed an increasing tendency in the presence of CP971P (Fig. 2). However, there was almost no difference in the PpIX fluorescence with 0.05% or 0.1% CP971P, but the uptake was higher with 0.1% CP971P. The presence of macromolecules in the culture medium may have been responsible for this. Since PpIX can only be formed in cells, there is no need to replace the culture medium after ALA incubation. In this study, after culturing with ALA (whether or not in the presence of CP971P), cells along with the culture medium were subjected to flow cytometric measurement without prewashing or replacing the medium. Therefore, the added CP971P was in the culture medium throughout the study. The effect of pharmaceutical excipients interfering with the measured absorbances of a drug was reported by Fuerte and Maldonado,[18] and predictions of the drug concentration in the analyzed samples can be misleading because of the scattering effect of light. Since light scattering can affect both the absorbance and the emission of light, one possible reason could be due to a light-scattering effect in the presence of macromolecules such as CP971P.

The cellular PpIX amount derived from ALA depends on ALA uptake and the activity of enzymes involved in ALA PpIX's conversion. ALA PDT-induced selective destruction of neoplastic lesions was attributed to an aberration of heme biosynthesis, such as the reduction of ferrochelatase activities or upregulation of porphobilinogen deaminase, in tumor cells.[16] As shown in Fig. 5, CP971 significantly increased the uptake of ALA in a concentration-dependent manner. Although 0.05% CP971 significantly increased the PpIX amount (Fig. 2), an increased concentration of CP971 did not further increase PpIX, which might

have been due to the maximum enzyme activity having already been achieved.

In conclusion, PDT is a new treatment modality for surface cancers such as skin cancers and oral cancers, and has shown potential in treating externally approachable sites. However, photosensitizers that can be used with PDT are extremely expensive. Although ALA, a photosensitizer precursor, is much less expensive than other photosensitizer drugs, it generally requires a larger dose and the cost is still rather high. To reduce the costs of PDT drugs, the field of excipient application is becoming more attractive. In this study, we proved that a mucoadhesive polymer, CP971P, can increase ALA uptake by cancer cells and the formation of PpIX.

Acknowledgments

This study was sponsored by a grant (SKH-TMU-93-05) from the Shin Kong Wu Ho-Su Memorial Hospital.

References

1. Malik Z, Lugaci H. Destruction of erythroleukaemic cells by photoactivation of endogenous porphyrins. *Br J Cancer* 1987;56:589–95.
2. Divaris DX, Kennedy JC, Pottier RH. Phototoxic damage to sebaceous glands and hair follicles of mice after systemic administration of 5-aminolevulinic acid correlates with localized protoporphyrin IX fluorescence. *Am J Pathol* 1990; 136:891–7.
3. Peng Q, Warloe T, Berg K, Moan J, Kongshaug M. 5-Aminolevulinic acid-based photodynamic therapy: clinical research and future challenges. *Cancer* 1997;79:2282–308.
4. Dolmans DE, Fukumura D, Jain RK. Photodynamic therapy for cancer. *Nat Rev Cancer* 2003;3:380–7.
5. Henderson BW, Dougherty TJ. How does photodynamic therapy work? *Photochem Photobiol* 1992;55:145–57.
6. Hillemanns P, Weingandt H, Baumgartner R, Diebold J, Xiang W, Stepp H. Photodetection of cervical intraepithelial neoplasia using 5-aminolevulinic acid-induced porphyrin fluorescence. *Cancer* 2000;88:2275–82.
7. Levulan Kerastick (aminolevulinic acid HCl) for topical solution, 20%. Available at: http://www.icare.org/fda.htm
8. Tsai JC, Chiang CP, Chen HM, et al. Photodynamic therapy of oral dysplasia with topical 5-aminolevulinic acid and light-emitting diode array. *Lasers Surg Med* 2004;34:18–24.
9. Chen HM, Chen CT, Yang H, et al. Successful treatment of oral verrucous hyperplasia with topical 5-aminolevulinic acid-mediated photodynamic therapy. *Oral Oncol* 2004;40: 630–7.
10. Yu CH, Chen HM, Hung HY, Cheng SJ, Tsai T, Chiang CP. Photodynamic therapy outcome for oral verrucous hyperplasia depends on the clinical appearance, size, color, epithelial dysplasia, and surface keratin thickness of the lesion. *Oral Oncol* 2008;44:595–600.
11. Chien HF, Liao YH, Chen CT. Topical 5-aminolevulinic acid photodynamic therapy for warts. *Lasers Surg Med* 2007; 39(S19):57.
12. Wang YS, Tay YK, Kwok C, Tan E. Photodynamic therapy with 20% aminolevulinic acid for the treatment of recalcitrant viral warts in an Asian population. *Int J Dermatol* 2007;46: 1180–4.
13. Duncan R. The dawning era of polymer therapeutics. *Nat Rev Drug Discov* 2003;2:347–60.
14. Pharmaceutical Ingredients. Lubrizol Web site. http://www.lubrizol.com/Pharmaceutical/default.html
15. Gerlier D, Thomasset N. Use of MTT colorimetric assay to measure cell activation. *J Immunol Methods* 1986;94:57–63.
16. Gibson SL, Nguyen ML, Havens JJ, Barbarin A, Hilf R. Relationship of delta-aminolevulinic acid-induced protoporphyrin IX levels to mitochondrial content in neoplastic cells in vitro. *Biochem Biophys Res Commun* 1999;265:315–21.
17. Masters JR. False cell lines: the problem and a solution. *Cytotechnology* 2002;39:69–74.
18. Fuerte V, Maldonado M, Rees GD. The multicomponent automated dissolution system: an alternative in the development and pharmaceutical analysis of generic polydrugs. *J Pharm Biomed Anal* 1999;21:267–72.

J Dent Sci 2010;5(1):36–40

CASE REPORT

Successful treatment of an early invasive oral squamous cell carcinoma with topical 5-aminolevulinic acid-mediated photodynamic therapy

*Hsin-Ming Chen,[1,2,3] Chuan-Hang Yu,[2] Hung-Pin Lin,[2] Hsiang Yang,[3] Ru-Cheng Kuo,[3] Ying-Shiung Kuo,[4] Chun-Pin Chiang[1,2,3]**

[1]Graduate Institute of Oral Biology, School of Dentistry, National Taiwan University, Taipei, Taiwan
[2]Graduate Institute of Clinical Dentistry, School of Dentistry, National Taiwan University, Taipei, Taiwan
[3]Department of Dentistry, National Taiwan University Hospital, College of Medicine, National Taiwan University, Taipei, Taiwan
[4]Department of Dentistry, Far Eastern Memorial Hospital, Taipei, Taiwan

Received: Nov 23, 2009
Accepted: Jan 21, 2010

KEY WORDS:
5-aminolevulinic acid;
early invasive oral cancer;
topical photodynamic therapy

Our previous studies showed successful treatment of a series of 36 oral verrucous hyperplasia lesions and of an extensive oral verrucous carcinoma with a topical 5-aminolevulinic acid (ALA)-mediated photodynamic therapy (topical ALA-PDT) protocol (with a fluence rate of 100 mW/cm^2 and a light exposure dose of 100 J/cm^2) using a 635-nm light-emitting diode (LED) light source. In this case report, we tested whether an enhanced topical ALA-PDT protocol (with a fluence rate of 200 mW/cm^2 and a light exposure dose of 200 J/cm^2) could be used to treat an early invasive oral squamous cell carcinoma (OSCC) with a verrucous appearance of the left lower posterior edentulous alveolar mucosa of a 67-year-old male former areca-quid chewer and ex-smoker. The main verrucous lesion showed complete regression after eight treatments with PDT. However, 10 extra treatments were needed to eradicate the multiple residual leukoplakia lesions on the edentulous alveolar mucosa. Moderate to severe post-PDT pain was noted during the initial eight treatments, and the patient needed analgesics (codeine phosphate, 30 mg three times daily) to control the pain. No recurrence of the OSCC lesion was found after a follow-up period of 4 years. We suggest that our enhanced topical ALA-PDT protocol may have good potential to be used as a treatment of choice for a superficially invasive OSCC without regional or distant metastasis before the commencement of other effective therapies.

Introduction

Oral cancer is the fifth most common cancer in the world.[1] In Taiwan, oral cancers ranked as the sixth most prevalent cancer in both sexes and was the fourth most common cancer in males in 2006.[2] The main etiologies of oral squamous cell carcinoma (OSCC) in Taiwan are areca quid (AQ) (betel nut,

*Corresponding author. Department of Dentistry, National Taiwan University Hospital, 1, Chang-Te Street, Taipei 10048, Taiwan.
E-mail: cpchiang@ntu.edu.tw

Areca catechu) chewing, cigarette smoking, and alcohol consumption. There are 2 million people who habitually chew AQ,[3] and approximately 80% of all oral cancer deaths are associated with this habit.[4] In Taiwan, oral cancers are usually treated with radical surgical excision, chemotherapy, and radiotherapy, separately or in combination. Although various treatment modalities are used, the survival rate for oral cancer patients in Taiwan remains low. The respective 5-year survival rates are 72%, 39%, 27%, and 12% for those with stage I, II, III, and IV oral cancers.[5] The low 5-year survival rate in patients with advanced oral cancers suggests the importance of early detection and treatment of oral cancers. In addition, one of the best strategies to prevent oral cancers is to identify the oral cancers at their precancerous stages or at as early a stage as possible and eliminate them to prevent their further transformation into oral cancers.

Oral verrucous carcinoma (OVC) is a low-grade but usually extensive tumor of the oral mucosa. An OVC may develop into an invasive OSCC during its late carcinogenic stage. Traditional treatment for OVC is total surgical excision that always leads to scar formation. Photodynamic therapy (PDT) is another effective treatment option for human premalignant and malignant lesions because it is noninvasive, is well tolerated by patients, can be used repeatedly without cumulative side effects, and results in little scar formation.[6] 5-Aminolevulinic acid (ALA) itself is not a photosensitizer but serves as the biological precursor of the photosensitizer, protoporphyrin IX (PpIX), in the heme biosynthesis pathway. PDT with topically applied ALA (topical ALA-PDT) is used for treatment of human oral premalignant lesions with relatively good clinical outcomes.[7–14] Our previous studies showed successful treatment of 36 oral verrucous hyperplasia (OVH) lesions and an extensive OVC with a topical ALA-PDT protocol (with a fluence rate of 100 mW/cm^2 and a light exposure dose of 100 J/cm^2) using a 635-nm light-emitting diode (LED) light source.[10–15] In this case report, we tested the efficacy of an enhanced topical ALA-PDT protocol (with a fluence rate of 200 mW/cm^2 and a light exposure dose of 200 J/cm^2) on an early invasive OSCC with a verrucous appearance at the buccal gingiva of tooth 33 and the edentulous alveolar mucosa of the teeth 34–36 region of a 67-year-old male former AQ chewer and ex-smoker.

Case presentation

This 67-year-old male patient was referred to our outpatient dental clinic for treatment of a verrucous lesion measuring about 3 × 1.5 cm on the buccal gingiva of tooth 33 and the edentulous alveolar mucosa of the teeth 34–36 region (Fig. 1A). The patient had hypertension (systolic pressure of 140 mmHg and diastolic pressure of 90 mmHg on average) that was under drug control. The patient denied having any other major systemic diseases. The patient had chewed AQ (40–50 quids/day) for 30 years and had smoked (20 cigarettes/day) for 40 years. He had quitted chewing AQ 10 years previously, but had only quitted smoking 4 months previously. He began to notice a verrucous tumor on the left lower posterior edentulous alveolar mucosal area 4 months previously. Although he had quitted smoking 4 months previously, the tumor continued to grow to the present form and size. During the past 4 months, the patient had received no treatment. Based on the size and appearance of the lesion, the tentative clinical diagnosis was an OVC. However, an incisional biopsy taken from the tumor portion of the edentulous alveolar mucosa of the tooth 34 area showed an early invasive OSCC (Figs. 1B and 1C). Magnetic resonance imaging revealed no metastatic lymph nodes in the bilateral submandibular, carotid or posterior cervical region. In addition, a whole-body bone scan revealed no bone metastasis. The patient refused to undergo wide surgical excision of the tumor. After discussion with the patient, we decided to use an enhanced topical ALA-PDT protocol (with a fluence rate of 200 mW/cm^2 and a light exposure dose of 200 J/cm^2) to treat him after he provided informed consent.

The treatment course for this patient was the same as that for our previous OVH or OVC patients as described previously,[10–15] except that a twofold higher light exposure dose was given to the patient in this case. In brief, at the first visit, an oral examination and incisional biopsy were performed. At the second appointment, we did a kinetics study with topical ALA using ALA-induced PpIX fluorescence spectroscopy and found that the PpIX reached its maximum level in the lesional epithelial cells 1.5 hours after local ALA application. Therefore, the subsequent light treatments were set at 1.5 hours after topical application of ALA to the lesion. The topical ALA-PDT was performed once a week beginning from the patient's third appointment. On the day of treatment, 0.8 mL of 20% ALA was applied to the entire tumor upon the patient's arrival. The light treatment was composed of multiple 3-minute sessions of irradiation with an LED red light at 635 ± 5 nm separated with several 3-minute rest periods for a total of 1000 seconds (with a fluence rate of 200 mW/cm^2 and a light exposure dose of 200 J/cm^2) which was delivered 1.5 hours after topical ALA application. Light treatments were carried out under local anesthesia using 2% lidocaine with the patient fully conscious. The tip of the LED light device was kept as close to the surface of the lesion as possible. The verrucous lesion showed nearly

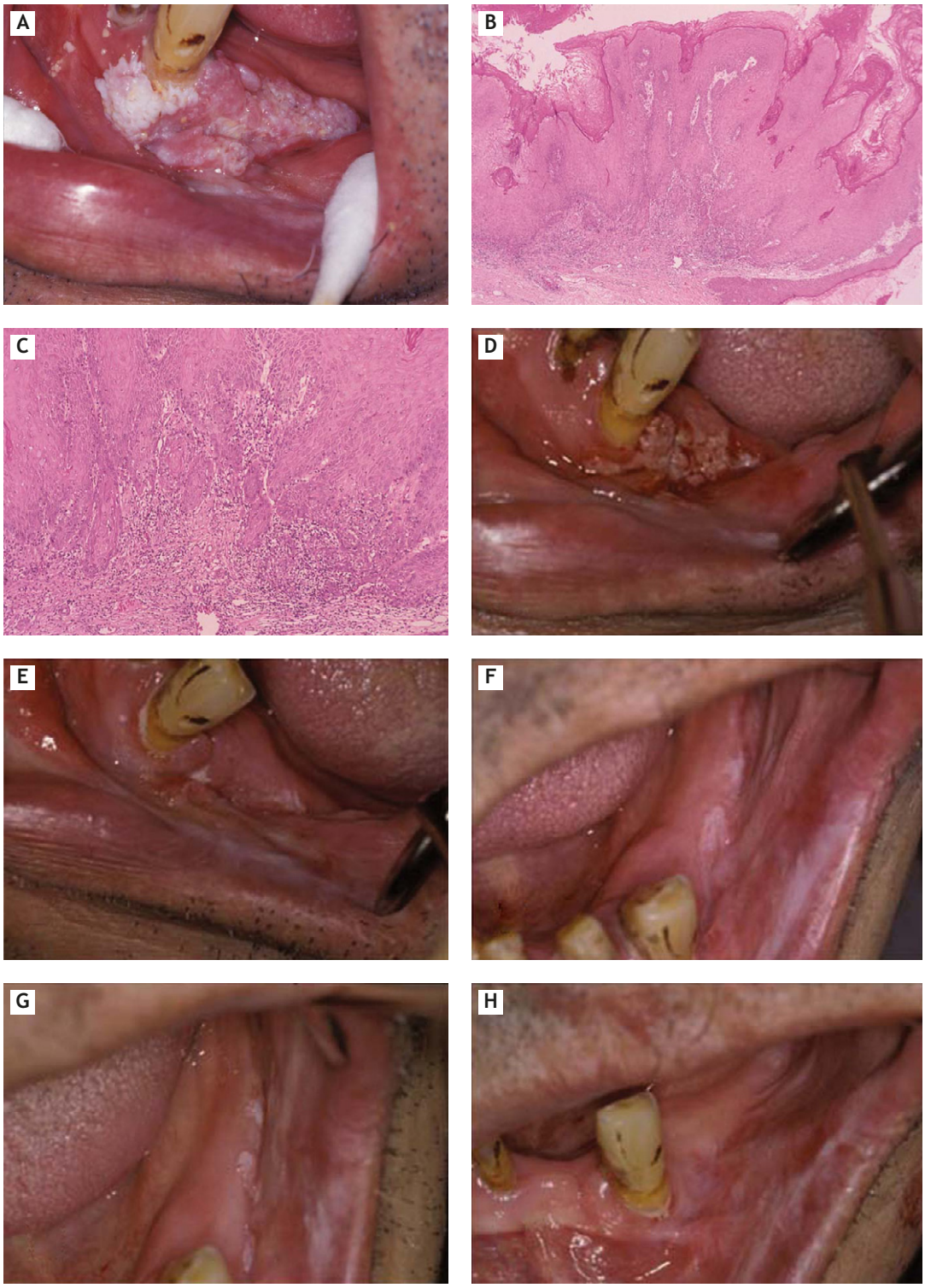

Fig. 1 Clinical photographs and histologic microphotographs of an early invasive squamous cell carcinoma (SCC) lesion. (A) An initial oral verrucous carcinoma-like lesion at the buccal gingiva of tooth 33 and the edentulous alveolar mucosa of the teeth 34–36 region before treatment. (B, C) Incisional biopsy of the tumor portion at the edentulous alveolar mucosa of the tooth 34 area showing a verrucous carcinoma with early invasion of SCC tumor nests into the underlying connective tissue (hematoxylin and eosin stain; B: original magnification ×5, C: original magnification ×25). Clinical photographs of the early invasive SCC lesion showing a partial response of the main verrucous lesion after (D) three and (E) six treatments of the enhanced topical ALA-PDT, nearly complete regression of the main verrucous lesion after (F) eight PDT treatments, multiple residual leukoplakic lesions at the edentulous alveolar mucosa after (F) eight and (G) 14 PDT treatments, and complete regression of the lesion after (H) 18 PDT treatments. (H) A white lesion of oral submucous fibrosis is still evident at the left buccal mucosa.

complete regression after eight treatments of the enhanced topical ALA-PDT (Figs. 1D–F). However, the multiple residual leukoplakia lesions needed 10 extra treatments to achieve complete regression (Figs. 1G and 1H). Because of the severe post-PDT pain, codeine phosphate (30 mg/tablet, 1 tablet 3 times/day) was prescribed for the patient for the former eight treatments and acetaminophen (500 mg/tablet, 1 tablet 4 times/day) was given to the patient for the latter 10 treatments after PDT. After completion of the entire treatment course, the patient was followed up once every 2 weeks in the 1st month, once every 2 months in the following 6 months, and once every 3 months thereafter. No recurrence of the lesion was found after a follow-up period of 4 years.

Discussion

In this case report, we describe treatment of an early invasive OSCC on the buccal gingiva of tooth 33 and the edentulous alveolar mucosa of the teeth 34–36 region of a 67-year-old male former AQ chewer and ex-smoker by a new enhanced topical ALA-PDT protocol. The early invasive OSCC lesion showed complete regression after a total of 18 treatments of topical ALA-PDT. In our previous studies, a topical ALA-PDT protocol was successfully used to treat 36 OVH lesions, an extensive OVC lesion, and an extensive OVH lesion.[10–16] The results of the present report confirmed that our new enhanced topical ALA-PDT protocol also has good potential as an effective treatment modality for superficially invasive OSCC lesions.

The clinical appearance and treatment course of this superficially invasive OSCC lesion were comparable to those of our previously reported extensive OVH lesion.[16] Both lesions had a verrucous appearance and showed complete regression after 18 treatments with enhanced topical ALA-PDT. The incubation period (the time needed for the transformation of ALA into PpIX) was 1.5 hours, and the total light exposure dose per treatment was 200 J/cm^2 for both lesions. In addition, both lesions demonstrated nearly complete regression after eight treatments of the enhanced topical ALA-PDT. This suggests that doubling the light dose may slightly shorten the treatment course compared with that for our previously reported extensive OVC case. However, more-severe post-PDT pain was experienced by this early invasive OSCC patient than by our previous OVC patient. Therefore, stronger analgesics were needed for this patient to control the post-PDT pain than for the previous OVC patient.

PDT with topically applied ALA is used to treat oral precancerous lesions like oral leukoplakia (OL) and OVH and cancerous lesions like OVC with promising clinical outcomes.[7–16] Kubler et al.[7] treated 12 OL lesions with PDT after local application of 20% ALA cream and found a complete response (CR) in five, a partial response (PR) in four, and no response (NR) in three. Sieron et al.[8,9] treated 17 OL lesions with PDT after topical application of 10% ALA ointment or emulsion in two separate studies. A CR was observed in 14 of 17 OL lesions. Our previous studies showed that complete regression of 36 OVH lesions was achieved with fewer than seven treatments of topical ALA-PDT once a week.[14] However, for an extensive OVC or OVH lesion, more treatments are needed.[15,16] Our previous studies revealed that topical ALA-PDT is not very effective for OL lesion. The 65 OL lesions treated with topical ALA-PDT once a week showed a CR in five, a PR in 33, and NR in 27. The 32 OL lesions treated with the same topical ALA-PDT twice a week demonstrated a CR in 11 and a PR in 21. The twice-a-week treatment modality had a better clinical outcome for OL lesions than the once-a-week modality.[13] The need for 10 treatments of PDT to eradicate the multiple residual OL lesions in this patients also indicates the relative difficulty of obtaining a CR with topical ALA-PDT with medium- and small-sized OVH lesions.[14] However, the results of the above-mentioned investigations suggest that PDT with topical ALA may be an effective treatment modality for OVH and OVC lesions and may have a good potential to be used as a treatment of choice for OVC and superficially invasive OSCC lesions without regional or distant metastasis. Further studies are needed to assess whether the new enhanced topical ALA-PDT is more effective than the previously used topical ALA-PDT for treating OL lesions.

The successful clinical outcome for this early invasive OSCC lesion treated by the new enhanced topical ALA-PDT may have been due to the ALA preparation, the specific topical ALA-PDT protocol used, and the characteristic clinical, histologic and biologic features of the lesion itself. The reasons why our specific ALA preparation and the topical ALA-PDT protocol used resulted in a successful clinical outcome for OVH lesions were previously described.[11–14,16] Similar reasons could be used to explain the successful clinical outcome for this case as well. The verrucous appearance of the present lesion provided a large area for good retention of ALA on the surface, and the less keratotic epithelium of this lesion than OL lesions also provided a more permeable surface layer for good absorption of ALA into the oral epithelial cells. Furthermore, malignant epithelial cells may retain more ALA than hyperplastic epithelial cells, and the thinner surface keratin layer may only have a minimal effect on reducing the light intensity. In addition, there are more epithelial cells in the cell division cycle in cancerous than in hyperplastic oral

lesions. Malignant epithelial cells in the cell division cycle are more susceptible to destruction by PDT-generated singlet oxygen molecules and free radicals than those epithelial cells not in the cell division cycle. The sufficient photosensitizer and light dose ultimately resulted in a good clinical outcome for this early invasive OSCC lesion.

In this case report, we succeeded in treating a superficially invasive OSCC with an enhanced protocol of topical ALA-PDT. Although further studies are needed to verify the true efficacy of this enhanced treatment protocol, we suggest that our enhanced topical ALA-PDT protocol has good potential to be used as a treatment of choice for an early invasive OSCC without regional or distant metastasis before the commencement of other effective therapies.

Acknowledgments

The authors would like to thank the Industrial Technology Research Institute, Hsin Chu, Taiwan, for developing the light-emitting diode source.

References

1. Lingen M, Sturgis EM, Kies MS. Squamous cell carcinoma of the head and neck in non-smokers: clinical and biologic characteristics and implications for management. *Curr Opin Oncol* 2001;13:176–82.
2. Cancer registry annual report in Taiwan area, 2006. Department of Health, The Executive Yuan, Taiwan, 2007.
3. Ko YC, Huang YL, Lee CH, Chen MJ, Lin LM, Tsai CC. Betel quid chewing, cigarette smoking and alcohol consumption related to oral cancer in Taiwan. *J Oral Pathol Med* 1995;24:450–3.
4. Kwan HW. A statistical study on oral carcinomas in Taiwan with emphasis on the relationship with betel nut chewing: a preliminary report. *J Formos Med Assoc* 1976;75:497–505.
5. Chen YK, Huang HC, Lin LM, Lin CC. Primary oral squamous cell carcinoma: an analysis of 703 cases in southern Taiwan. *Oral Oncol* 1999;35:173–9.
6. Dolmans DE, Fukumura D, Jain RK. Photodynamic therapy for cancer. *Nat Rev Cancer* 2003;3:380–7.
7. Kubler A, Haase T, Rheinwald M, Barth T, Muhling J. Treatment of oral leukoplakia by topical application of 5-aminolevulinic acid. *Int J Oral Maxillofac Surg* 1998;27:466–9.
8. Sieron A, Namyslowski G, Misiolek M, Adamek M, Kawczyk-Krupka A. Photodynamic therapy of premalignant lesions and local recurrence of laryngeal and hypopharyngeal cancers. *Eur Arch Otorhinolaryngol* 2001;258:349–52.
9. Sieron A, Adamek M, Kawczyk-Krupka A, Mazur S, Ilewicz L. Photodynamic therapy (PDT) using topically applied δ-aminolevulinic acid (ALA) for the treatment of oral leukoplakia. *J Oral Pathol Med* 2003;32:330–6.
10. Tsai JC, Chiang CP, Chen HM, et al. Photodynamic therapy of oral dysplasia with topical 5-aminolevulinic acid and light-emitting diode array. *Lasers Surg Med* 2004;34:18–24.
11. Chen HM, Chen CT, Yang H, et al. Successful treatment of oral verrucous hyperplasia with topical 5-aminolevulinic acid-mediated photodynamic therapy. *Oral Oncol* 2004;40:630–7.
12. Chen HM, Yu CH, Tu PC, Yeh CY, Tsai T, Chiang CP. Successful treatment of oral verrucous hyperplasia and oral leukoplakia with topical 5-aminolevulinic acid-mediated photodynamic therapy. *Lasers Surg Med* 2005;37:114–22.
13. Chen HM, Yu CH, Tsai T, Hsu YC, Kuo RC, Chiang CP. Topical 5-aminolevulinic acid-mediated photodynamic therapy for oral verrucous hyperplasia, oral leukoplakia, and oral erythroleukoplakia. *Photodiagnosis Photodyn Ther* 2007;4:44–52.
14. Yu CH, Chen HM, Hung HY, Cheng SJ, Tsai TM, Chiang CP. Photodynamic therapy outcome for oral verrucous hyperplasia depends on the clinical appearance, size, color, epithelial dysplasia, and surface keratin thickness of the lesion. *Oral Oncol* 2008;44:595–600.
15. Chen HM, Chen CT, Yang H, et al. Successful treatment of an extensive verrucous carcinoma with topical 5-aminolevulinic acid-mediated photodynamic therapy. *J Oral Pathol Med* 2005;34:253–6.
16. Chen HM, Yu CH, Chang JYF, Tsai T, Kuo RC, Chiang CP. Successful treatment of an extensive oral verrucous hyperplasia with topical 5-aminolevulinic acid-mediated photodynamic therapy—case report. *J Dent Sci* 2007;2:216–20.

J Dent Sci 2010;5(1):41–46

CASE REPORT

Dramatic recovery from severe anemia by resolution of severe periodontitis

Shin-Yu Lu,[1] Hock-Liew Eng[2]*

[1]Department of Oral Pathology and Family Dentistry, Chang Gung Memorial Hospital, Kaohsiung Medical Center, Chang Gung University College of Medicine, Kaohsiung, Taiwan
[2]Department of Pathology, Chang Gung Memorial Hospital, Kaohsiung Medical Center, Chang Gung University College of Medicine, Kaohsiung, Taiwan

Received: Nov 2, 2009
Accepted: Feb 19, 2010

KEY WORDS:
anemia of chronic disease;
periodontitis

Periodontal infections were previously found to be associated with systemic diseases such as diabetes, stroke, cardiovascular disease, bacterial pneumonia, and preterm low births. Individuals with gum disease have increased concentrations of circulating inflammatory markers that contribute to systemic inflammation, and periodontitis may tend towards anemia because of depressed erythropoiesis. Anemia of chronic disease (ACD) is defined as anemia that occurs during infections, inflammation, neoplasia, and a wide range of diseases including renal, endocrine and cardiovascular diseases. The etiology of ACD is multifactorial, but is often under-recognized and undertreated. This article describes an unusual case of severe anemia caused by severe periodontitis in a 50-year-old woman. After extracting many hopeless teeth, resolving the periodontitis and making new dentures, a dramatic recovery from the severe anemia was obvious 4 months later, and her health-related quality of life vastly improved. All blood values returned to normal with no medication. Chronic periodontitis can be a cause of ACD. The diagnosis of ACD based on the mean size and heterogeneity of red blood cells and an iron study, such as serum iron and ferritin, is discussed.

Introduction

Periodontitis was found to have a relationship with a number of systemic health conditions, including diabetes, stroke, cardiovascular disease, and pneumonia.[1–4] An otherwise healthy population with severe periodontitis has high inflammatory markers of C-reactive protein (CRP) and interleukin (IL)-6. The more severe periodontitis is, the higher serum concentrations of inflammatory markers that exist[5]. In addition, the severe type of periodontitis induces chronic inflammation and an immune reaction which depresses erythropoiesis and results in anemia.[6] Chronic periodontitis can be a definite cause of anemia of chronic disease (ACD). ACD commonly occurs with chronic infections, inflammation, autoimmune diseases, cancers, and chronic kidney diseases.[7,8] Therefore, ACD has been called many things, such as anemia of inflammation, anemia of infection, anemia of malignancy, anemia of defective iron utilization, and anemia of renal disease. This anemia is characterized by decreased plasma iron and

*Corresponding author. Department of Oral Pathology and Family Dentistry, Chang Gung Memorial Hospital, 123, Da-Pi Road, Niaosong Township, Kaohsiung County 83301, Taiwan.
E-mail: jasminelu@adm.cgmh.org.tw

iron-binding capacity, impaired release of reticuloendothelial iron into the plasma, a modest decrease in red blood cell (RBC) survival, and relative failure of bone marrow to increase RBC production.[9] Their clinical similarities were the reason that these anemias were classified into a single category, ACD.

ACD is often mistaken for iron-deficiency anemia (IDA), because low serum iron and decreased transferrin saturation are found in both conditions. A major condition associated with ACD is the marked dysregulation of iron homeostasis by a reticuloendothelial block rather than a true iron deficiency. The differential diagnosis between ACD and IDA is very important to avoid unnecessary iron replacement therapy. Because the etiology of ACD is multifactorial, there is no specific therapy for ACD. If its underlying cause is found and treated successfully, the anemia will resolve immediately.

Periodontitis is very common clinically, but there are very few case reports demonstrating the direct causal relationship between periodontitis and ACD. Dental practitioners and medical doctors often ignore the oral manifestations and changes in the RBC distribution width (RDW) and mean corpuscular volume (MCV) until the hemoglobin level is very low. Therefore, a rare case in which severe chronic periodontitis resulted in ACD is described in this article. After the periodontitis was resolved, all blood values returned to normal ranges, and the patient completely recovered from ACD. A detailed oral examination in the investigation of patients with unexplainable ACD is necessary and important. This case report provides valuable evidence on this subject.

Case presentation

A 50-year-old woman required assistance from her two sons to visit the dental department of Kaohsiung Chang Gung Memorial Hospital because of weakness, difficulty in chewing foods, and teeth mobility over a 2-year period. The patient looked debilitated but denied having any systemic diseases (Fig. 1A). One year before her dental visit, she had consulted a family medicine department with the complaint of general weakness and limited walking ability. At that time during a routine check, the hematologic study revealed anemia, but no definite diagnosis was made and no special therapy was given. The laboratory data given 1 year before her dental visit showed a white blood cell (WBC) count of $5.3\times10^3/\mu L$, an RBC count of $2.95\times10^6/\mu L$, hemoglobin (Hb) of 9.1 g/dL, an MCV of 93.7 fL, hematocrit (Hct) of 27.7%, standard deviation of red cell distribution width (RDW-SD) of 49.0 fL, a platelet count of $254\times10^3/\mu L$, ferritin of 108 ng/mL, serum iron of 39 μg%, total iron-binding capacity (TIBC) of 172 μg%, folate of 4.5 ng/mL, vitamin B_{12} of 480 pg/mL, normal blood sugar, normal renal and hepatic function, but increased CRP, and mildly decreased albumin (Table 1, column 3). Due to her worsening condition of cachexia and loss of body weight, she was forced to accept dental treatment, but still hesitated because of irrational fears to face dentists, the so-called dentophobia. She admitted that fear of the situation often brought on a panic attack or severe anxiety.

A detailed oral examination and panoramic check revealed extremely poor oral hygiene, heavy

Table 1. Laboratory data of a 50-year-old woman with anemia of chronic disease

Item	1 year before the dental visit	At the dental visit	After transfusing 4 packs of RBCs	Normal range
WBC (/μL)	5.3×10^3	5.1×10^3	5.5×10^3	$3.5–11\times10^3$
RBC (/μL)	2.95×10^6	2.49×10^6	3.84×10^6	$4–5.2\times10^6$
Hb (g/dL)	9.1	7.6	11.6	12–16*
MCV (fL)	93.7	87.1	92.4	80–100
MCH (pg/cell)	30.8	30.5	30.2	26–34
Hct (%)	27.7	21.7	35.5	36–46
RDW-SD (fL)	49.0	39.8	46.9	38–45
Plt (/μL)	254×10^3	251×10^3	26.7×10^3	$150–400\times10^3$
Ferritin (ng/mL)	108	126	–	28 (6–142)
Fe (μg%)	39	32	–	40–150
TIBC (μg%)	172	156	–	250–400
Fe/TIBC (%)	22.7	20.5		
Folate (ng/mL)	4.5	4.2	–	>2.5
Vitamin B_{12} (pg/mL)	480	399	–	160–970

*The degree of anemia was scaled by the Hb level as mild (Hb, 10.0 g/dL to normal limits), moderate (Hb, 8.0–9.9 g/dL), severe (Hb, 6.5–7.9 g/dL), and life-threatening anemia (Hb, <6.5 g/dL). WBC = white blood cell; RBC = red blood cell; Hb = hemoglobin; MCV = mean corpuscular volume; MCH = mean corpuscular hemoglobin; Hct = hematocrit; RDW = red cell distribution width; SD = standard deviation; Plt = platelet; Fe = iron; TIBC = total iron-binding capacity.

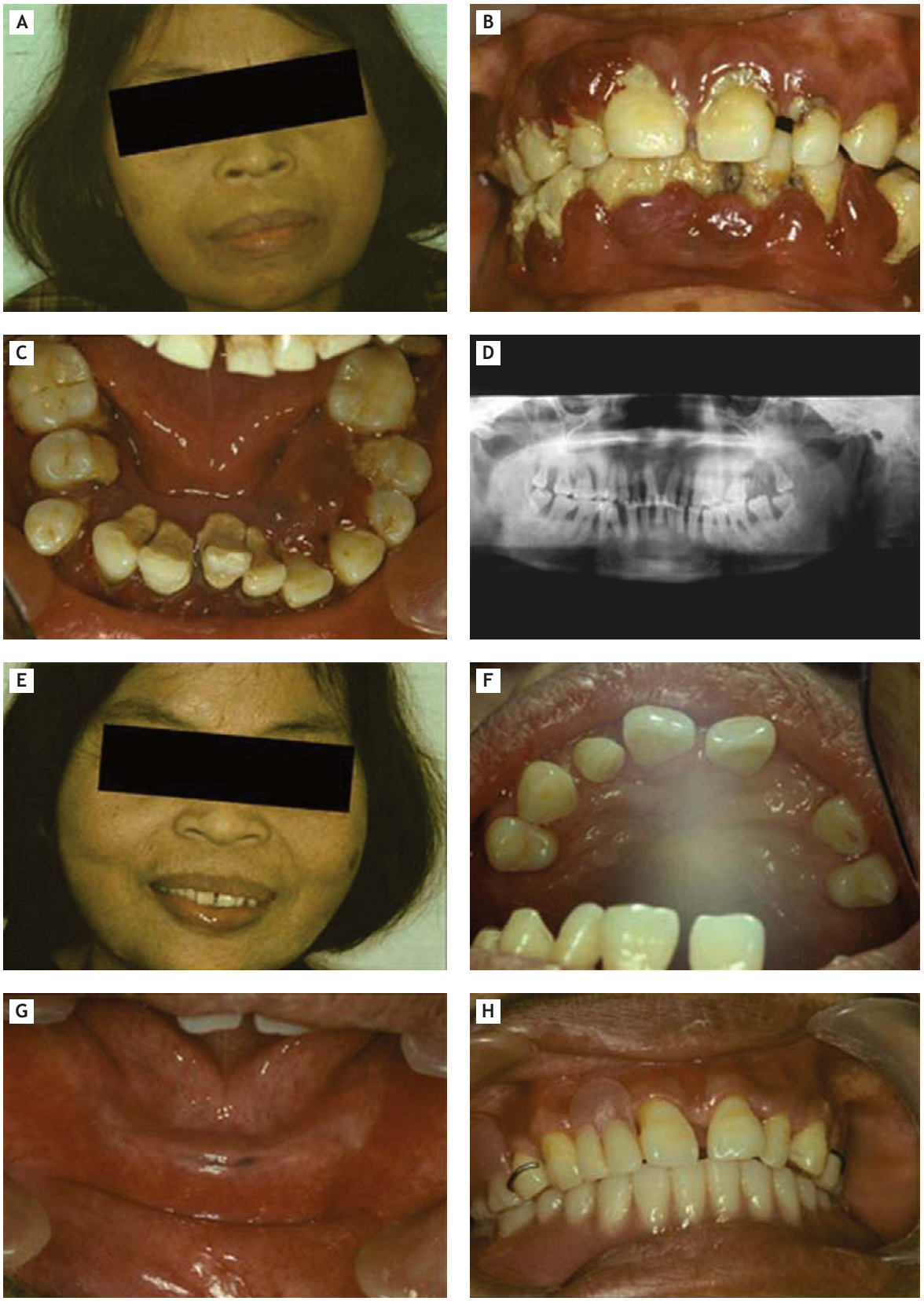

Fig. 1 (A–D) A 50-year-old debilitated woman with severe anemia who suffered from gum swelling and high mobility of many teeth over a 2-year period. Heavy calculus deposition, teeth migration, and severe alveolar bone destruction were noted in the panoramic radiographs. (E–H) Dramatic recovery of the severe anemia, improvement in the quality of life, and body weight gain were obvious 4 months after radical periodontal therapy, extraction of 21 hopeless teeth, and delivery of new dentures.

calculus deposition, severe gingival swelling, moderate to severe alveolar bone loss, and periodontitis with high mobility of many teeth that resulted in difficulty in chewing foods and oral hygiene maintenance (Figs. 1B–D). Rechecking the complete blood count (CBC) and micronutrients showed a WBC count of $5.1 \times 10^3/\mu L$, an RBC count of $2.49 \times 10^6/\mu L$, Hb of 7.6 g/dL, an MCV of 87.1 fL, Hct of 21.7%, an RDW-SD of 39.8 fL, a platelet count of $251 \times 10^3/\mu L$, ferritin of 126 ng/mL, serum iron of 32 μg%, a TIBC of 156 μg%, folate of 4.2 ng/mL, and vitamin B_{12} of 399 pg/mL (Table 1, column 4). According to a comparison between columns 3 and 4 of Table 1, the anemia had progressively worsened over the past year, but no obvious reason was found. After consultation with a hematologist, a bone marrow biopsy from the posterior iliac crest was performed to demonstrate increased erythropoiesis in response to severe anemia. After all systemic diseases and malignancy were excluded, severe periodontitis was proposed as the possible cause of the anemia.

In trying to relieve the patient of her dentophobia, we made great efforts to gain her confidence and let her feel relaxed during communication and the examination. Since the patient's family hoped to finish all dental treatment within a few appointments, we suggested extracting 21 teeth and performing radical periodontal treatment with a blood transfusion and general anesthesia in one visit, and then making new dentures to improve mastication 2 weeks later. They accepted the proposal and decided the date of the operation. Four units of packed RBCs were transfused prior to surgery so that the Hb immediately increased to 11.6 g/dL. The patient tolerated the operation well and had no complications. The pathologic study of the excised gingival tissues showed severe gum hyperplasia and inflammation (Fig. 2).

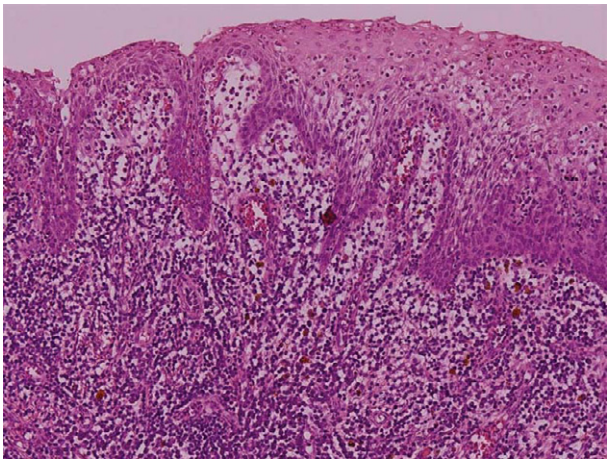

Fig. 2 Histologic features of the excised gingival tissue showing severe gingival hyperplasia and inflammation. (hematoxylin and eosin, 66×)

A new denture insertion was delivered 2 months later (Figs. 1F–H), so that the patient could eat without any difficulty. Dramatic recovery of ACD with CBC and CRP returning to normal ranges with no medication was obvious 4 months after the operation. Thereafter, she was able to establish confidence in dentists and ameliorate her dentophobia. The patient subjectively felt much improvement in her quality of life including increased happiness, physical agility, and body weight gain (Fig. 1E).

Discussion

The relationship between oral infections and systemic diseases has to do with periodontal disease.[1–4] Human periodontal and endodontic infections are associated with complex microflora in which hundreds of species are predominately gram-negative anaerobes. The anatomic closeness of these microflora to the bloodstream can facilitate transient bacteremia and systemic spread of bacterial products, components, and immunocomplexes. From available studies, it appears that compared with a healthy control group, the total number of leukocytes and plasma level of CRP are consistently higher, but the RBC count and level of Hb are lower in periodontitis groups.[5,6] This means that the periodontitis group possesses a trend towards ACD. ACD, the second most prevalent anemia to IDA, often occurs in patients with chronic renal or cardiovascular diseases, chronic infections, inflammation, and neoplasia. ACD usually coexists with the presence of adequate iron stores and vitamins. Because the etiologies, mechanisms and pathogenesis of ACD are not clearly delineated, their boundaries are indefinite. To the present, ACD is defined by its clinical and laboratory features, so there are no precise diagnostic criteria. The possible mechanisms of ACD include decreased RBC survival, an impaired erythropoietic response to anemia by ineffective erythropoiesis or existing inhibitors, and decreased utilization of reticuloendothelial iron for Hb synthesis.

The major pathophysiology of ACD is due to the inability of macrophages to release iron which normally comes from the breakdown of senescent RBCs, so serum iron falls while the iron stores are normal or increased. From Table 2, a conclusion can be drawn that ACD is characterized by decreased serum iron, decreased transferrin saturation (serum iron over TIBC), and increased ferritin. The plasma TIBC is usually normal or low in ACD but increased in IDA, although this is not sufficiently reliable to distinguish these two disorders. For ACD, the decrease in transferrin saturation primarily reflects the decreased level of serum iron. But for IDA, transferrin

Table 2. Iron-related characteristics of typical anemia of chronic disease (ACD) and iron-deficiency anemia (IDA)

Item	ACD	IDA
Fe	Low	Low
TIBC	Normal or low	High
Transferrin saturation (Fe/TIBC)	Low	Much lower
Ferritin	High	Low

Fe = serum iron; TIBC = total iron-binding capacity.

saturation may be even lower because TIBC is increased. Therefore, ACD may be mistaken for IDA, because low serum iron and decreased transferrin saturation are found in both conditions. Under such a situation, serum ferritin is the unique noninvasive test to differentiate ACD from IDA.[8,9] It is important to note that ACD should be carefully distinguished from IDA to avoid unnecessary iron replacement therapy.

By referring to column 4 of Table 1, it is clear that at her first dental visit, the CBC data of this patient revealed severe anemia (Hb, 7.6 g/dL) and severely low Hct (21.7%) but homogenous normocytosis (normal MCV and RDW). Generally, the degree of anemia in ACD is often mild with Hct levels within the range of 30–40%.[10,11] Sometimes as in this case, anemia in ACD may be more severe with the Hct below 25%.[11,12] ACD is usually normochromic (normal Hct) and normocytic (normal MCV), but may be hypochromic (low Hct) and microcytic (low MCV).[12] In terms of timing, hypochromia always precedes microcytosis in ACD, which is in contrast to the situation with IDA.[10,13] In ACD patients, the RDW, an assessment of heterogeneity of red cell volume, was also found to be either normal or increased.[13,14] Therefore, the anemia of ACD is not well classified with MCV or RDW.[15,16] For the patient in this case report, the transferrin saturation (Fe/TIBC) changed from 22.7% to 20.5%, and ferritin was always $>$100 ng/mL during the entire year before her dental visit. As a general rule, an MCV of $<$70 fL, transferrin saturation of $<$16%, and serum ferritin of $<$20 ng/mL are only found in IDA.[13] These data greatly differ from those in ACD (an MCV rarely $<$70 fL, transferrin saturation of $>$16%, and a high serum ferritin of $>$50 ng/mL). A comparison of this patient's hematologic features (Table 1, columns 3 and 4) showed that the hypochromia was getting worse, and moderate anemia with heterogeneous normocytosis was shifting to severe anemia with homogenous normocytosis during the previous year. As a result of these findings, ACD was determined to be an existing condition.

The increased CRP and increased ferritin reflected the correlation between ACD and chronic infection. After all systemic diseases and malignancy were excluded, chronic infection resulting from severe periodontitis was the only possible etiology of ACD in this case. Iron is an essential nutrient for proliferating microorganisms. The sequestration of iron from microorganisms to the reticuloendothelial system is believed to be a potentially effective defense strategy to inhibit the growth of pathogens[17]. Proinflammatory cytokines, such as IL-6, IL-1 and TNF-α, divert iron from the circulation to the reticuloendothelial system in lymph nodes and spleen. This process is facilitated through increased erythrophagocytosis, increased production of ferritin, increased uptake of ferrous iron, and reduced release of iron by macrophages, and finally results in a reticuloendothelial block.[7,8] The reticuloendothelial block also stops the supply of iron and results in its side effect, ACD. However, the blockage of reticuloendothelial iron release in the pathogenesis of ACD remains to be further explored.

If possible, curing the underlying disease is the best therapy for ACD. Treating ACD is associated with a relatively poor prognosis among patients with cancer, chronic renal disease, and congestive heart failure. The severe anemia in the patient in this case report dramatically recovered after extracting many hopeless teeth and resolving the periodontitis. Normally, a blood transfusion is not necessary, because the degree of anemia in ACD is not severe enough to produce symptoms. For the sake of the patient's dentophobia, general weakness from severe anemia and the emergent need for radical dental care, we planned a single-stage treatment by removing 21 hopeless teeth and surgical periodontal flap therapy with deep curettage and root planning of all remaining teeth with a blood transfusion and general anesthesia. A blood transfusion with packed RBCs can provide rapid and effective therapy for promoting the patient's general status in a short period of time and speeding the healing of an operative wound. The general anesthesia procedure decreased the patient's fears, and the cardiovascular reaction was in a safer condition which favored the surgical intervention. Complete recovery of the severe anemia and improvements in the health-related quality of life were obvious 4 months later. All blood values returned to normal with no medication.

Relevant research suggests that decreased erythropoietin production plays an important role in anemia due to infection, inflammation or malignancy.[18] Progress in understanding the pathophysiology of ACD has improved the therapeutic strategies, including treatment of the underlying disease and the use of erythropoietic agents or blood transfusions. One is advised to remember that treating

ACD should include checking and proving all supposed etiologic factors, whenever they are possible and available.

This case report provides a good example of the direct causal relationship between periodontitis and ACD. It is very important to consider periodontitis as one of the possible etiologies of ACD during medical screening, when no other explainable causes are obvious. If identified during medical screening, the ACD can dramatically be improved by successful treatment of the underlying periodontitis.

References

1. Beck J, Garcia R, Heiss G, Vokonas PS, Offenbacher S. Periodontal disease and cardiovascular disease. *J Periodontol* 1996;67:1123–37.
2. Ebersole JL, Machen RL, Steffen MJ, Willmann DE. Systemic acute-phase reactants, C-reactive protein and heptoglobin, in adult periodontitis. *Clin Exp Immunol* 1997;107:347–52.
3. Li X, Kolltveit KM, Tronstad L, Olsen I. Systemic diseases caused by oral infection. *Clin Microbiol Rev* 2000;13:547–58.
4. Taylor BA, Tofler GH, Carey HMR, et al. Full-mouth tooth extraction lowers systemic inflammatory and thrombotic markers of cardiovascular risk. *J Dent Res* 2006;85:74–8.
5. Aiuto FD, Parkar M, Andreou G, et al. Periodontitis and systemic inflammation: control of local infection is associated with a reduction in serum inflammatory markers. *J Dent Res* 2004;83:156–60.
6. Hutter JW, Velden Uvd, Varoufaki A, Huffels RAM, Hoek FJ, Loos BG. Lower numbers of erythrocytes and lower levels of hemoglobin in periodontitis patients compared to control subjects. *J Clin Periodontol* 2001;28:930–6.
7. Weiss G. Pathogenesis and treatment of anemia of chronic disease. *Blood Rev* 2002;16:87–96.
8. Weiss G, Goodnough LT. Anemia of chronic disease. *N Eng J Med* 2005;352:1011–23.
9. Cartwright GE, Lee GR. The anaemia of chronic disorders. *Br J Haematol* 1971;21:147–52.
10. Mulherin D, Skelly M, Saunder A, et al. The diagnosis of iron deficiency in patients with rheumatoid arthritis and anemia; an algorithm using simple laboratory measures. *J Rheumatol* 1996;23:237–40.
11. Cash JM, Sears DA. The anemia of chronic disease: Spectrum of associated diseases in a series of unselected hospitalized patients. *Am J Med* 1989;87:638–44.
12. Chernow B, Wallner SF. Is the anemia of chronic disorders normocytic-normochromic? *Mil Med* 1978;143:345–6.
13. Bessman JD, Gilmer PR Jr, Gardner FH. Improved classification of anemias by MCV and RDW. *Am J Clin Pathol* 1983;80:322–6.
14. Garry PJ, Goodwin JS, Hunt WE. Iron status and anemia in the elderly: new findings and a review of previous studies. *J Am Geriatr Soc* 1983;31:389–99.
15. Lu SY, Wu HC. Initial diagnosis of anemia from sore mouth and improved classification of anemias by MCV and RDW in 30 patients. *Oral Surg Oral Med Oral Pathol Oral Radiol Endod* 2004;98:679–85.
16. Lu SY, Wang MC, Eng HL. Initial diagnosis of B12 deficiency from sore mouth and assessment of their RDW, MCV and hemoglobin in 34 patients. *J Dent Sci* 2006;1:23–31.
17. Weinberg ED. Iron loading and disease surveillance. *Emerg Infect Dis* 1999;5:346–52.
18. Zucker S, Friedman S, Lysik RM. Bone marrow erythropoiesis in the anemia of infection, inflammation, and malignancy. *J Clin Invest* 1974;53:1132–8.